Supplementary Information

Tunable self-assembly hierarchical superstructures of benzene-1,3,5-tricarboxamide-containing fullerene block molecules: from flower to urchin and rod-like morphologies

Luoxiao Sang, Huan Chen, Weiwei Qin, Xiaohong Li, Huanjun Lu, Sheng Wang* and Yingfeng Tu*

L. Sang, H. Chen, W. Qin, X. Li, S. Wang, Y. Tu

Jiangsu Key Laboratory of Advanced Functional Polymer Design and Application, College of Chemistry, Chemical Engineering and Materials Science, Soochow University, Suzhou 215123, China.

E-mail: wangsheng@suda.edu.cn; tuyingfeng@suda.edu.cn

H. Lu

Jiangsu Key Laboratory for Micro and Nano Heat Fluid Flow Technology and Energy Application, School of Physical Science and Technology, Suzhou University of Science and Technology, Suzhou 215009, China.

Table of Contents

1. Experimental Section

1.1 Materials

10-Amino-1-decanol (≥ 98.0%), 8-amino-1-octanol (≥ 97.0%), 6-amino-1-hexanol (≥ 97%), *n*-tetradecylamine (99%), *n*-dodecylamine (98%), *n*-decylamine (98%), *n*-octylamine (99%), *n*-hexylamine (99%) and 1,3,5-benzenetricarboxylic chloride (TMC, > 98%) (all from Macklin), 4-(dimethylamino)pyridine (DMAP, 99%), *N*,*N*-diisopropylearbodiimide (DIPC, 99%) (all from Alfa Aesar), *p*-toluenesulfonic acid (PTSA, 99%) (from J&K Chemical). [60]Fullerene (99.9%) was purchased from Yongxin Technology Co., Ltd (Henan, China). [60]Fullerenoacetic acid was synthesized according to the reported references.[1,2] All other chemicals were commercially available and were used as received.

1.2 Instrumentations

^{1}H and ^{13}C NMR spectra were obtained on an Agilent Direct-Drive Π 600 MHz NMR spectrometer (600 MHz ^{1}H and 150 MHz ^{13}C Larmor frequency). The chemical shifts (δ values) were measured in parts per million (ppm) down-field from tetramethylsilane (TMS) as an internal reference.

Matrix-assisted laser desorption/ionization time-of-flight (MALDI-TOF) mass spectra were acquired on a GCT-Primier mass spectrometer. Trans-2-[3-(4-tert-butylphenyl)-2-methyl-2-propenylidene]malononitrile (DCTB) and dithranol served as matrix and was prepared in $CHCl_3$ at a concentration of 20 mg/mL. Sodium iodide (NaI) served as cationizing agent and was prepared in methanol at a concentration of 10 mg/mL.

UV-Vis absorption spectra were measured on a Cary 60 UV-vis spectrophotometer.

FT-IR were measured on an IRTracer-100 infrared spectrometer.

Thermal gravimetric analysis (TGA) was carried out on a TG/DTA 6300 with a heating rate of 10 °C/min in nitrogen atmosphere.

Transmission electron microscopy (TEM) was performed on a HT7700 microscope, operating at a 120 kV accelerating voltage and liquid nitrogen temperature. TEM samples

for characterization of morphology were prepared by drop-casting a 5 mg/mL solution of toluene/isopropanol mixture onto copper grids (300 mesh) and draining the excess solution.

Scanning electron microscope (SEM) images was performed on a S-4700 field emission microscope, operating at a 0.5-30 kV accelerating voltage and liquid nitrogen temperature. SEM samples for characterizing the morphology were prepared by drop-casting a 5 mg/mL solution of the toluene/isopropanol mixture onto the silicon wafer and blotting out the excess solution.

Energy dispersive spectrometry (EDS) analysis was performed on a HITACHI SU8010 microscope equipped with an OCTANE SUPER energy spectrum detector.

Atomic force microscopy (AFM) images were carried out on a MultiMode 8 Atomic Force Microscope (Bruker Veeco) in PeakForce QNM mode in air, and two kinds of SNL Si_3N_4 cantilever (spring constant: 0.35 N/m, resonance frequency: 50-80 kHz and spring constant: 0.12 N/m, resonance frequency: 16-28 kHz) were used for measurements.

Grazing incidence wide-angle X-ray scattering (GI-WAXS) experiments were performed on Xeuss 3.0 with a Cu Kα source (λ = 1.54 Å). A Dectris 2R 1M detector was used to capture the scattering patterns and was situated at 150-300 mm from samples. Typical GIWAXS patterns were taken at an incidence angle of 0.3°. The GI-WAXS samples for detecting were prepared by drop-coating about 5 mg/mL of the solution onto a precleaned and treated silicon wafer and blotting out the excess solution.

1.3 Synthesis of C_{60}-C_m-C_n

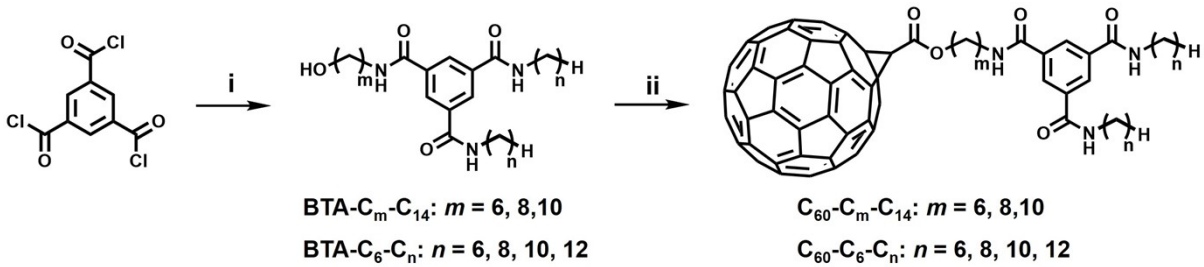

Scheme S1. Synthetic route to C_{60}-C_m-C_n. *Reagents and Conditions*: (i) $HO(CH_2)_mNH_2$, $H(CH_2)_nNH_2$, dichloromethane, triethylamine, 0 °C-r.t., 24 h, yield: 20-26%; (ii) [60]fullerenoacetic acid, DMAP, DIPC, PTSA, dichlorobenzene, DMF, r.t., 12 h, yield: 52-70 %.

BTA-C_{10}-C_{14}: Tetradecylamine (2.50 g, 11.6 mmol) was added to a mixture of 10-amino-1-decanol (1.00 g, 5.8 mmol) in dichloromethane and triethylamine, then placed in ice water with stirring. A dichloromethane solution of benzene-1,3,5-tricarbonyl chloride (1.40 g, 5.3 mmol) was added dropwise to the reaction, the mixture was stirred for 24 h at the room temperature, then concentrated under reduced pressure. The crude product was purified by column chromatography on silica gel (eluent: dichloromethane/ethyl acetate = 3/1, v/v), then concentrated under reduced pressure. Dried under vacuum to obtain a colorless transparent viscous oily liquid with a yield of 26%. ^{1}H NMR (600 MHz, $CDCl_3$, δ, ppm): 8.35 (d, Ar, 2H), 8.33 (d, Ar, 1H), 6.83 (d, NH, 2H), 6.66 (s, NH, 1H), 3.63 (td, CH_2, 2H), 3.43 (dd, CH_2, 6H), 1.89 (s, CH_2, 2H), 1.74 (s, CH_2, 2H), 1.59 (dt, CH_2, 6H), 1.56 – 1.48 (m, CH_2, 2H), 1.39 – 1.20 (m, CH_2, 54H), 0.87 (td, CH_3, 6H). ^{13}C NMR (151 MHz, $CDCl_3$, δ, ppm): 165.93, 135.18, 128.03, 62.90, 40.41, 40.25, 32.70, 31.91, 29.76 – 29.57, 29.55, 29.51, 29.35, 29.23, 29.13, 28.99, 27.02, 26.75, 25.57, 22.68, 14.11. MALDI-TOF: Calc. for $C_{47}H_{85}O_4N_3$: $[M+Na]^+$ 778.644. Found: 778.353.

BTA-C_8-C_{14}. ^{1}H NMR (600 MHz, $CDCl_3$, δ, ppm): 8.37 (t, Ar, 2H), 8.35 (s, Ar, 1H), 6.76 (t, NH, 3H), 3.63 (td, CH_2, 2H), 3.44 (dd, CH_2, 6H), 1.83 – 1.20 (m, CH_2, 60H), 0.88 (t, CH_3, 6H). ^{13}C NMR (151 MHz, $CDCl_3$, δ, ppm): 165.97, 135.19, 128.10, 62.75, 40.41, 40.19, 32.55, 31.91,

29.75 – 29.60, 29.56, 29.51, 29.35, 29.27, 28.99, 28.93, 27.04, 26.58, 25.44, 22.67, 14.10. MALDI-TOF: Calc. for $C_{45}H_{81}O_4N_3$: $[M+Na]^+$ 750.612 Found: 750.445.

BTA-C_6-C_{14}. ^{1}H NMR (600 MHz, $CDCl_3$, *δ*, ppm): 8.36 – 8.28 (m, Ar, 3H), 7.06 (s, NH, 1H), 6.93 (s, NH, 2H), 3.66 – 3.60 (m, CH_2, 2H), 3.48 – 3.37 (m, CH_2, 6H), 2.24 (s, OH, 2H), 1.64 – 1.48 (m, CH_2, 8H), 1.46 – 1.15 (m, CH_2, 48H), 0.87 (t, CH_3, 6H). ^{13}C NMR (151 MHz, $CDCl_3$, *δ*, ppm): 166.29, 135.22, 129.67 – 126.83, 62.38, 40.43, 40.02, 32.18, 31.91, 29.75 – 29.55, 29.50, 29.35, 29.08, 27.06, 26.36, 25.24, 22.68, 14.10. MALDI-TOF: Calc. for $C_{43}H_{77}O_4N_3$: $[M+Na]^+$ 772.581. Found: 772.507.

BTA-C_6-C_{12}. ^{1}H NMR (600 MHz, $CDCl_3$, *δ*, ppm): 8.33 (d, Ar, 2H), 8.31 (s, Ar, 1H), 7.07 (s, NH, 1H), 6.94 (s, NH, 2H), 3.64 (t, CH_2, 2H), 3.43 (dd, CH_2, 6H), 2.44 (s, OH, 1H), 1.66 – 1.50 (m, CH_2, 8H), 1.44 – 1.17 (m, CH_2, 40H), 0.88 (t, CH_3, 6H). ^{13}C NMR (151 MHz, $CDCl_3$, *δ*, ppm): 166.33, 135.23, 128.11, 62.38, 40.42, 40.02, 32.20, 31.90, 29.63, 29.49, 29.35, 29.08, 27.06, 26.37, 25.25, 22.67, 14.10. MALDI-TOF: Calc. for $C_{39}H_{69}O_4N_3$: $[M+Na]^+$ 666.519. Found: 666.208.

BTA-C_6-C_{10}. ^{1}H NMR (600 MHz, $CDCl_3$, *δ*, ppm): 8.27 (d, Ar, 3H), 7.07 (d, NH, 3H), 3.61 (t, CH_2, 2H), 3.39 (dd, CH_2, 6H), 2.39 (s, OH, 1H), 1.77 – 1.17 (m, CH_2, 40H), 0.87 (t, CH_3, 6H). ^{13}C NMR (151 MHz, $CDCl_3$, *δ*, ppm): 166.28, 135.21, 128.12, 62.38, 40.42, 40.01, 32.18, 31.87, 29.57, 29.48, 29.34, 29.30, 29.07, 27.04, 26.35, 25.23, 22.66, 14.09. MALDI-TOF: Calc. for $C_{35}H_{61}O_4N_3$: $[M+Na]^+$ 610.456. Found: 610.397.

BTA-C_6-C_8. ^{1}H NMR (600 MHz, $CDCl_3$, *δ*, ppm): 8.36 (d, Ar, 2H), 8.33 (d, Ar, 1H), 7.11 (s, NH, 1H), 6.97 (s, NH, 2H), 3.63 (q, CH_2, 2H), 3.41 (tt, CH_2, 6H), 2.21 (d, OH, 1H), 1.64 – 1.48 (m, CH_2, 8H), 1.39 – 1.22 (m, CH_2, 24H), 0.88 (t, CH_3, 6H). ^{13}C NMR (151 MHz, $CDCl_3$, *δ*, ppm): 166.31, 135.22, 128.14, 62.39, 40.42, 40.02, 32.19, 31.79, 29.48, 29.28, 29.20, 29.09, 27.03, 26.37, 25.25, 22.62, 14.07. MALDI-TOF: Calc. for $C_{31}H_{53}O_4N_3$: $[M+Na]^+$ 554.393. Found: 553.994.

BTA-C_6-C_6. ^{1}H NMR (600 MHz, $CDCl_3$, *δ*, ppm): 8.28 (t, Ar, 3H), 7.15 (s, NH, 2H), 3.65 – 3.56 (m, CH_2, 2H), 3.40 (dt, CH_2, 6H), 2.46 (s, OH, 2H), 1.56 (ddd, CH_2, 8H), 1.32 (dq, CH_2, 16H), 0.88 (t, CH_3, 6H). ^{13}C NMR (151 MHz, $CDCl_3$, *δ*, ppm): 166.39, 135.22, 128.15, 62.36, 40.40,

40.03, 32.20, 31.48, 29.41, 29.09, 26.68, 26.38, 25.25, 22.54, 14.01. MALDI-TOF: Calc. for $C_{27}H_{45}O_4N_3$: $[M+Na]^+$ 498.331. Found: 498.208.

C_{60}-C_{10}-C_{14}: BTA-C_{10}-C_{14} (0.46 g, 0.61 mmol) was added to a mixture of [60]fullerenoacetic acid (0.47 g, 0.60 mmol) in 1,2-dichlorobenzene and DMF, then added DMAP (0.22 g, 1.8 mmol), PTSA (0.32 g, 1.8 mmol) and DIPC (0.75 g, 2.4 mmol). The mixture was stirred at room temperature for 12 h, then filtered and concentrated under reduced pressure. The crude product was purified by column chromatography on silica gel (eluent: dichloromethane/methanol = 200/1, v/v), then concentrated under reduced pressure. The residue was precipitated in methanol, filtered and dried under vacuum to obtain a kermesinus solid with a yield of 64%. ^{1}H NMR (600 MHz, $CDCl_3$, δ, ppm): 8.34 (s, Ar, 3H), 6.49 (s, NH, 3H), 4.80 (s, CH, 1H), 4.47 (t, CH_2, 2H), 3.47 (s, CH_2, 6H), 1.90-1.83 (m, CH_2, 2H), 1.62 (d, CH_2, 6H), 1.55-1.49 (m, CH_2, 2H), 1.42-1.24 (m, CH_2, 54H), 0.88 (t, CH_3, 6H). MALDI-TOF: Calc. for $C_{109}H_{85}O_5N_3$: $[M+Na]^+$ 1538.639. Found: 1538.594.

C_{60}-C_8-C_{14}. ^{1}H NMR (600 MHz, $CDCl_3$, δ, ppm): 8.34 (d, Ar, 3H), 6.49-6.41 (m, NH, 3H), 4.80 (s, CH, 1H), 4.47 (t, CH_2, 2H), 3.51-3.44 (m, CH_2, 6H), 1.91-1.84 (m, CH_2, 2H), 1.67-1.16 (m, CH_2, 58H), 0.88 (t, CH_3, 6H). MALDI-TOF: Calc. for $C_{109}H_{85}O_5N_3$: $[M+Na]^+$ 1510.607. Found: 1510.646.

C_{60}-C_6-C_{14}. ^{1}H NMR (600 MHz, $CDCl_3$, δ, ppm): 8.34 (d, Ar, 3H), 6.50 (d, NH, 3H), 4.81 (s, CH_2, 1H), 4.49 (t, CH_2, 2H), 3.49 (ddd, CH_2, 6H), 1.90 (dt, CH_2, 2H), 1.73-1.21 (m, CH_2, 67H), 0.88 (t, CH_3, 6H). MALDI-TOF: Calc. for $C_{105}H_{77}O_5N_3$: $[M+Na]^+$ 1482.576. Found: 1482.796.

C_{60}-C_6-C_{12}. ^{1}H NMR (600 MHz, $CDCl_3$, δ, ppm): 8.34 (d, Ar, 3H), 6.46 (d, NH, 3H), 4.81 (s, CH, 1H), 4.49 (t, CH_2, 2H), 3.49 (ddd, CH_2, 6H), 1.94-1.87 (m, CH_2, 2H), 1.73-1.15 (m, CH_2, 46H), 0.88 (t, CH_3, 6H). MALDI-TOF: Calc. for $C_{101}H_{69}O_5N_3$: $[M+Na]^+$ 1426.513. Found: 1426.757.

C_{60}-C_6-C_{10}. ^{1}H NMR (600 MHz, $CDCl_3$, δ, ppm): 8.34 (dd, Ar, 3H), 6.44 (dd, NH, 3H), 4.81 (s, CH, 1H), 4.49 (t, CH_2, 2H), 3.49 (ddd, CH_2, 6H), 1.94-1.86 (m, CH_2, 2H), 1.75-1.21 (m, CH_2, 38H), 0.88 (t, CH_3, 6H). MALDI-TOF: Calc. for $C_{97}H_{61}O_5N_3$: $[M+Na]^+$ 1370.451. Found: 1375.948.

C_{60}-C_6-C_8. ^{1}H NMR (600 MHz, $CDCl_3$, δ, ppm): 8.35 (t, Ar, 3H), 6.49 (d, NH, 3H), 4.81 (s, 1H), 4.49 (t, CH_2, 2H), 3.49 (ddd, CH_2, 6H), 1.96-1.15 (m, CH_2, 32H), 0.88 (t, CH_2, 6H). MALDI-TOF: Calc. for $C_{93}H_{53}O_5N_3$: $[M+Na]^+$ 1314.388. Found: 1314.445.

C_{60}-C_6-C_6. ^{1}H NMR (600 MHz, $CDCl_3$, δ, ppm): 8.35 (d, Ar, 3H), 6.48 (dt, NH, 3H), 4.81 (s, CH, 1H), 4.49 (t, CH_2, 2H), 3.50 (ddd, CH_2, 6H), 1.93-1.88 (m, CH_2, 2H), 1.73-1.18 (m, CH_2, 22H), 0.90 (t, CH_3, 6H). MALDI-TOF: Calc. for $C_{89}H_{45}O_5N_3$: $[M+Na]^+$ 1258.326. Found: 1258.068.

1.4 Preparation of hierarchical superstructures

To a 3 mL sample bottle, 5 mg of fullerene derivative and 1 mL toluene/isopropanol mixed solvent was added and heated until the solid was completely dissolved. This solution was then aged at room temperature for above 12 h. The obtained hierarchical superstructures were then sent to TEM, SEM, AFM and 2D SAXS measurements.

2. Supporting Figures

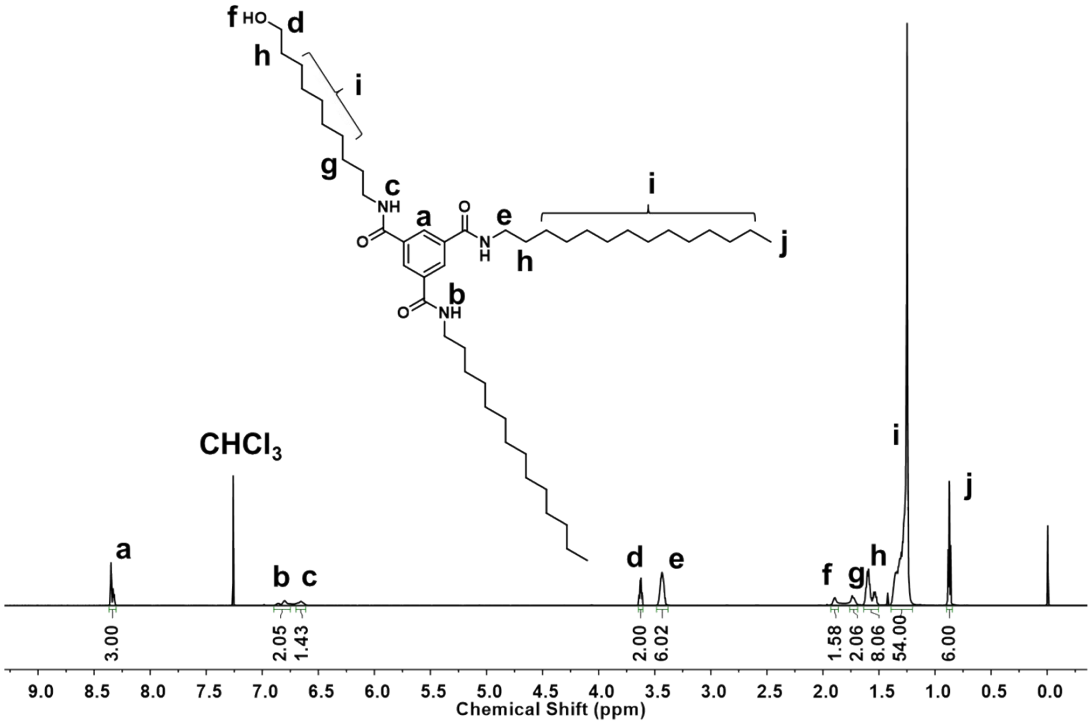

Fig. S1 ^{1}H NMR spectrum of BTA-C_{10}-C_{14}.

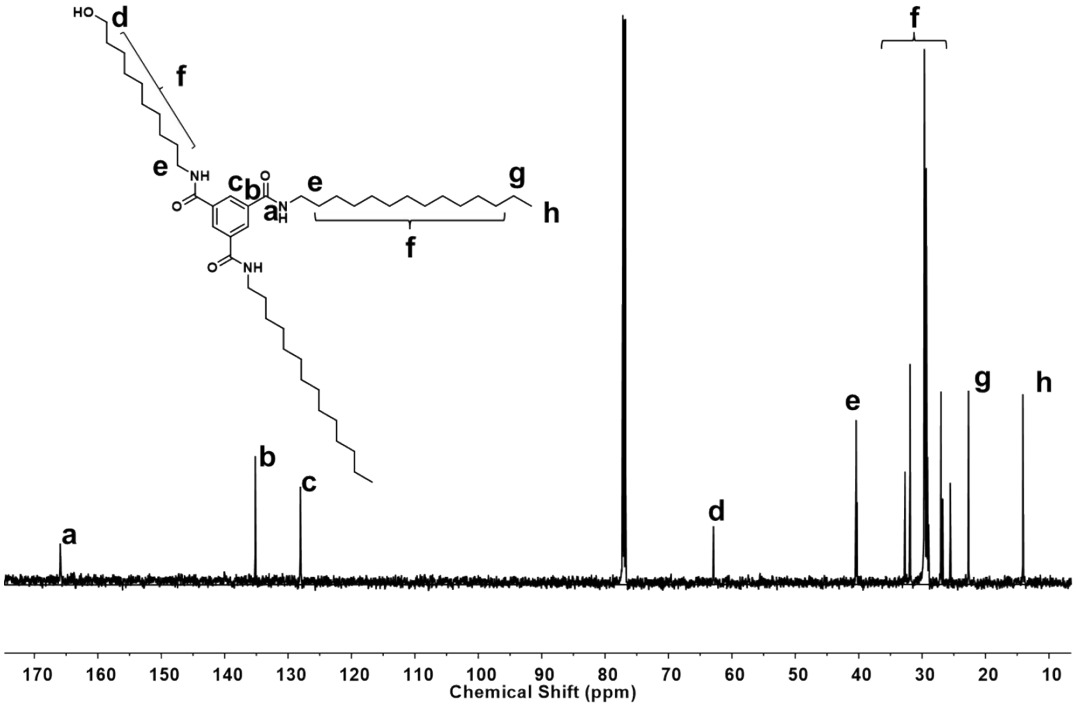

Fig. S2 ^{13}C NMR spectrum of BTA-C_{10}-C_{14}.

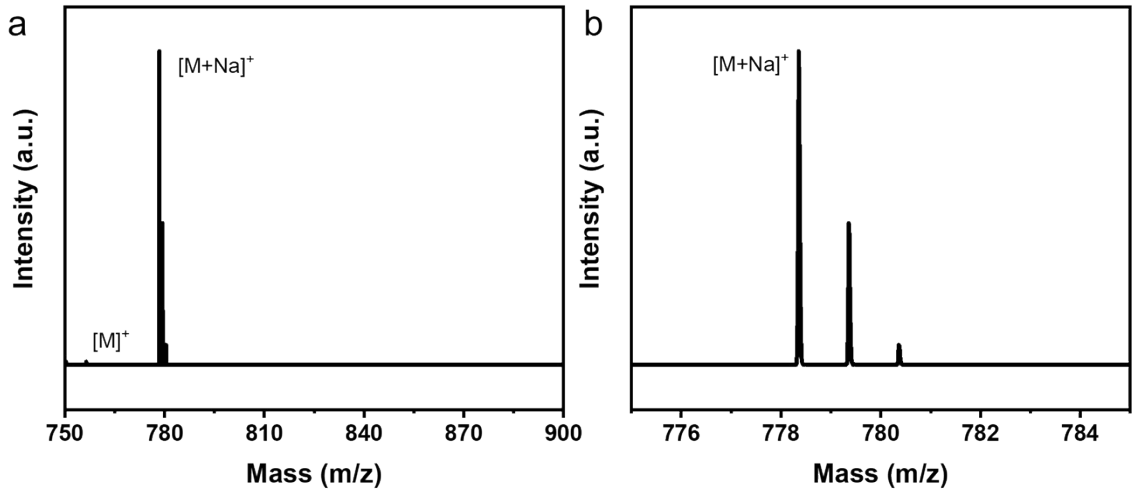

Fig. S3 MALDI-TOF mass spectra of BTA-C_{10}-C_{14}. (a) The overview of the spectrum and (b) the zoom-in view of the spectrum.

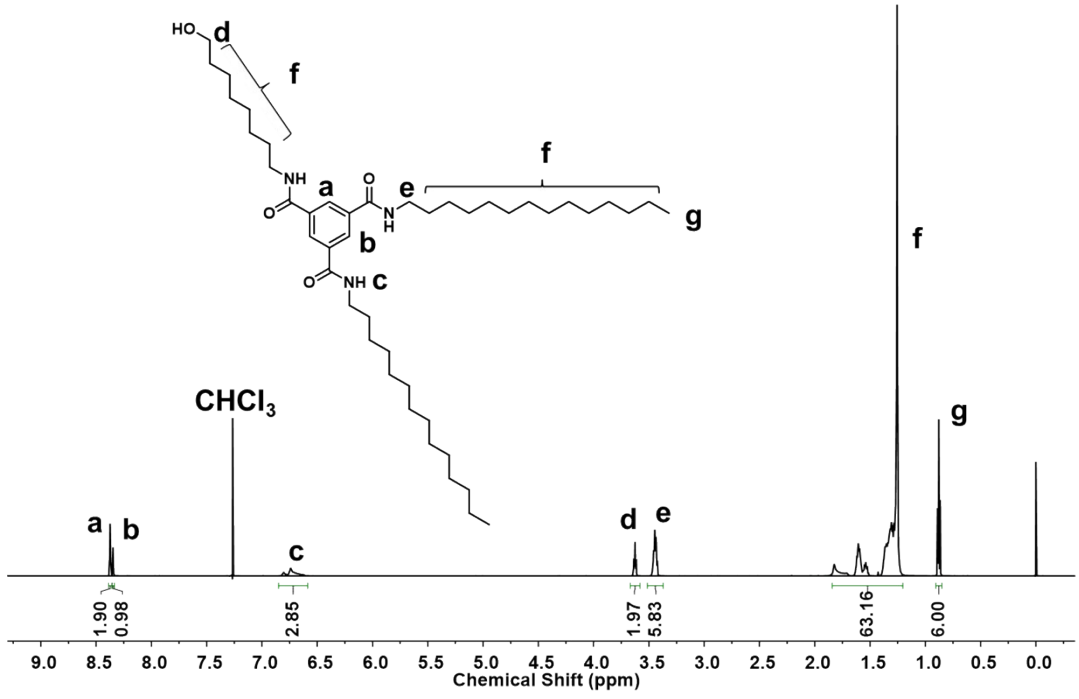

Fig. S4 ^{1}H NMR spectrum of BTA-C_8-C_{14}.

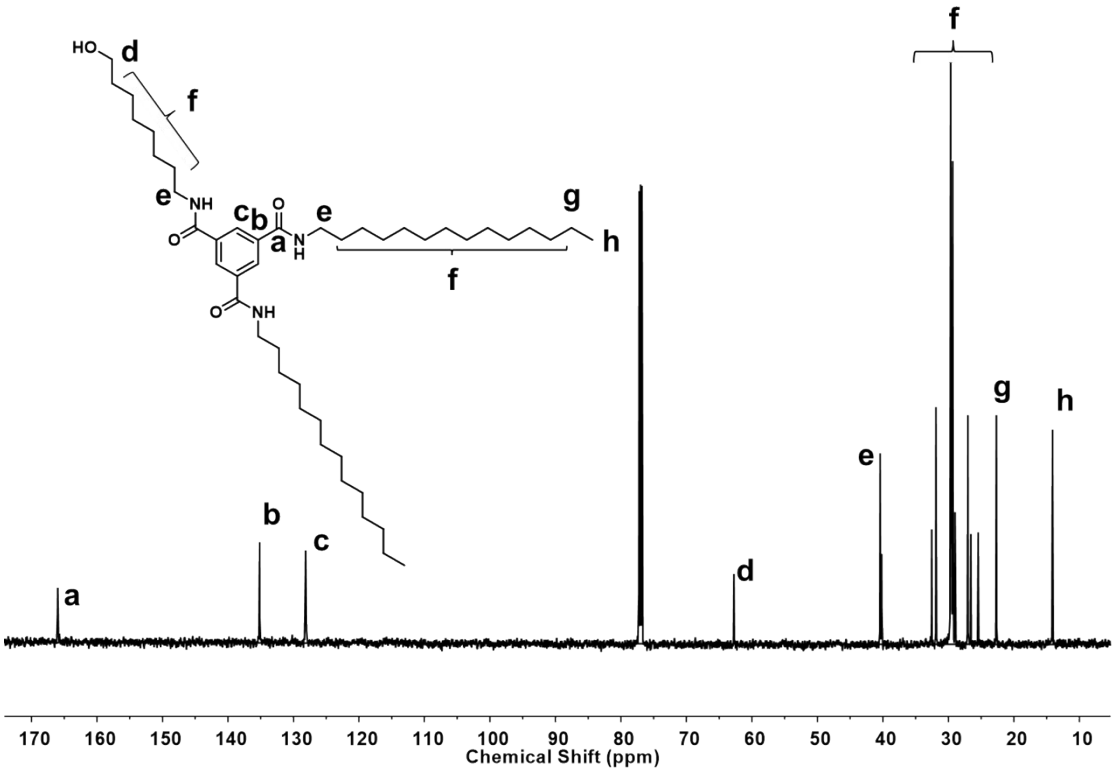

Fig. S5 ^{13}C NMR spectrum of BTA-C_8-C_{14}.

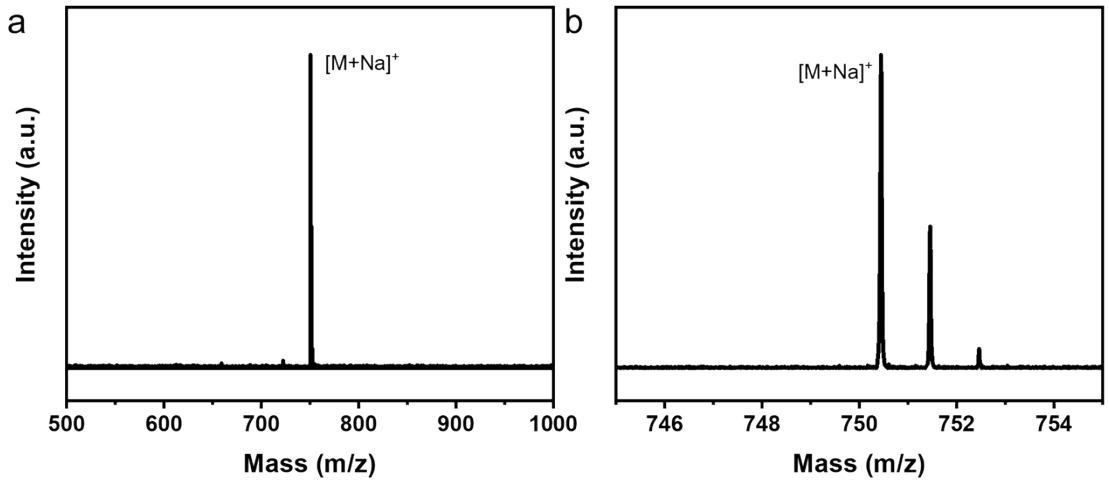

Fig. S6 MALDI-TOF mass spectra of BTA-C_8-C_{14}. (a) The overview of the spectrum and (b) the zoom-in view of the spectrum.

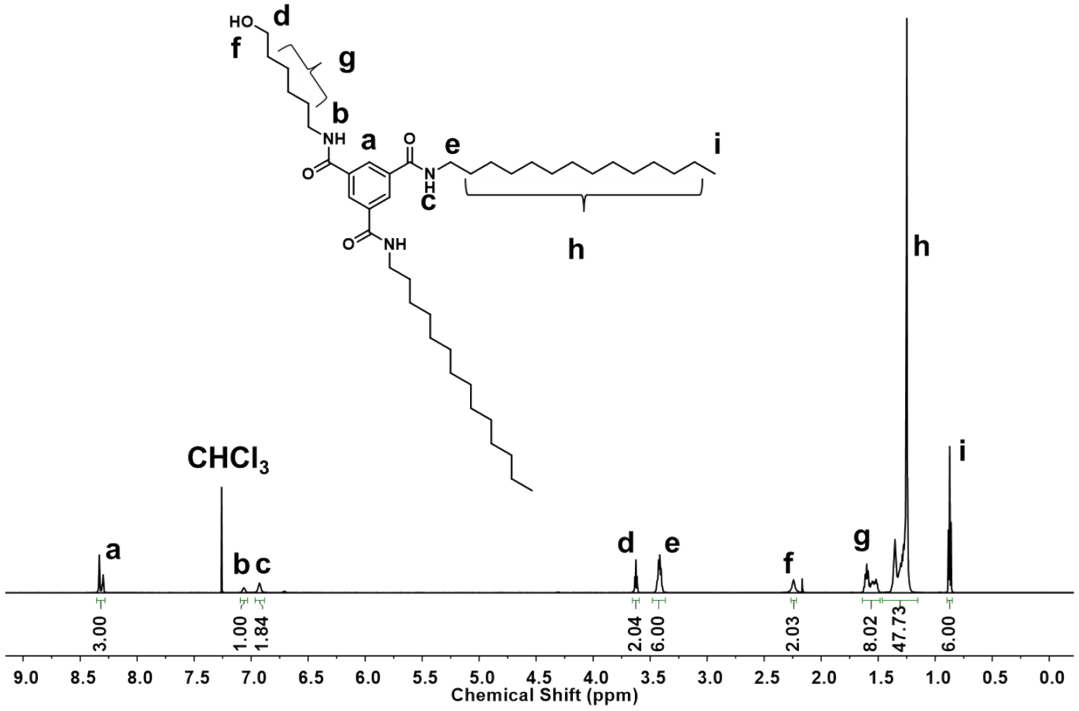

Fig. S7 ^{1}H NMR spectrum of BTA-C_6-C_{14}.

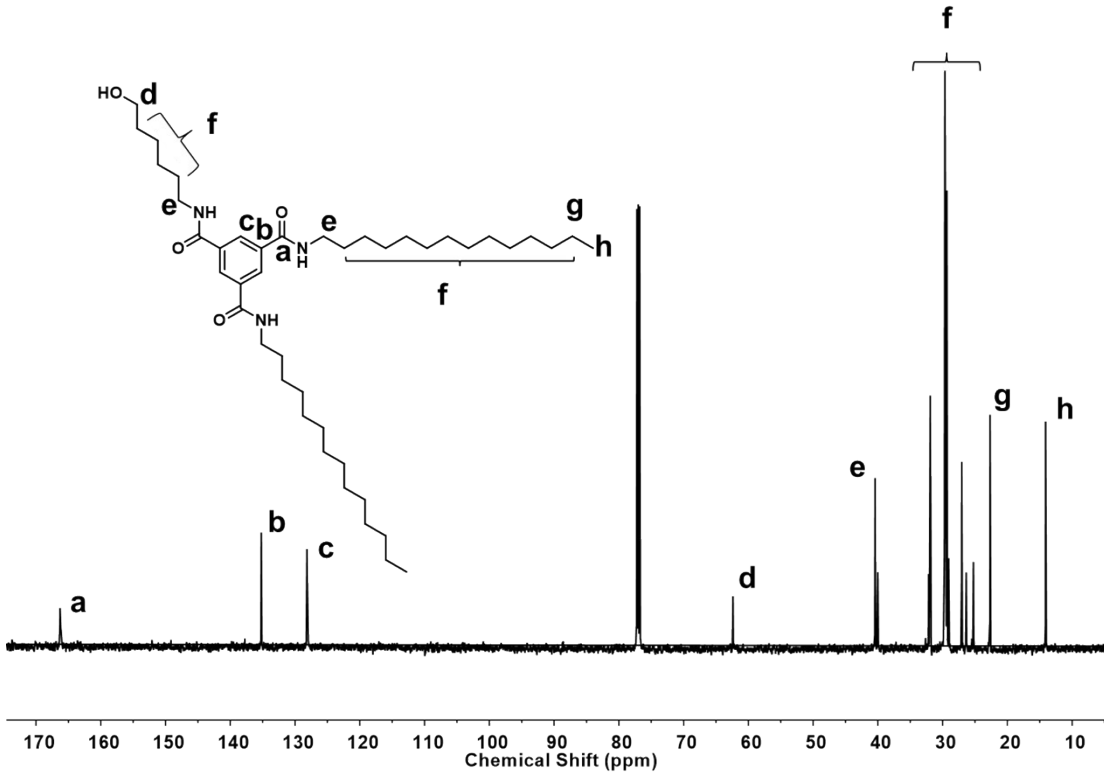

Fig. S8 ^{13}C NMR spectrum of BTA-C_6-C_{14}.

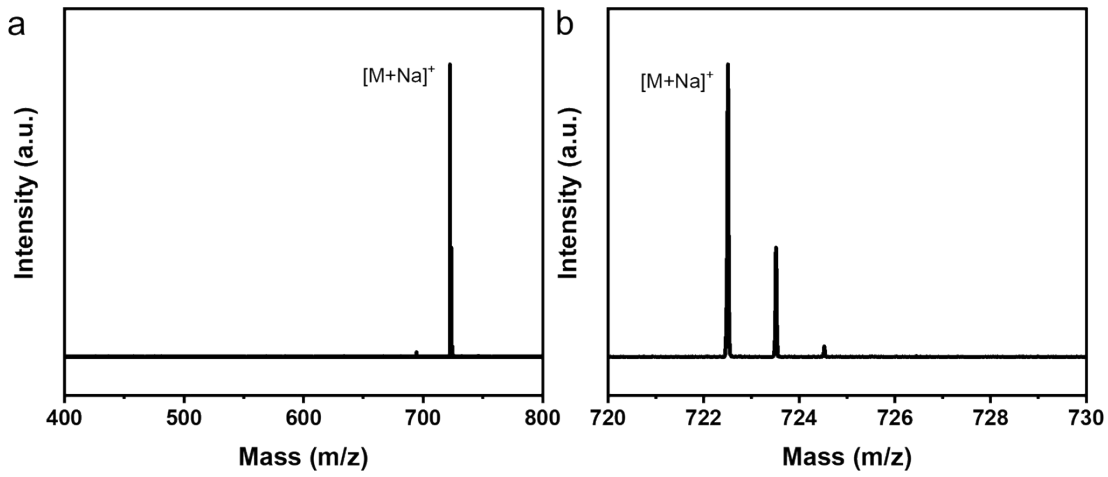

Fig. S9 MALDI-TOF mass spectra of BTA-C_6-C_{14}. (a) The overview of the spectrum and (b) the zoom-in view of the spectrum.

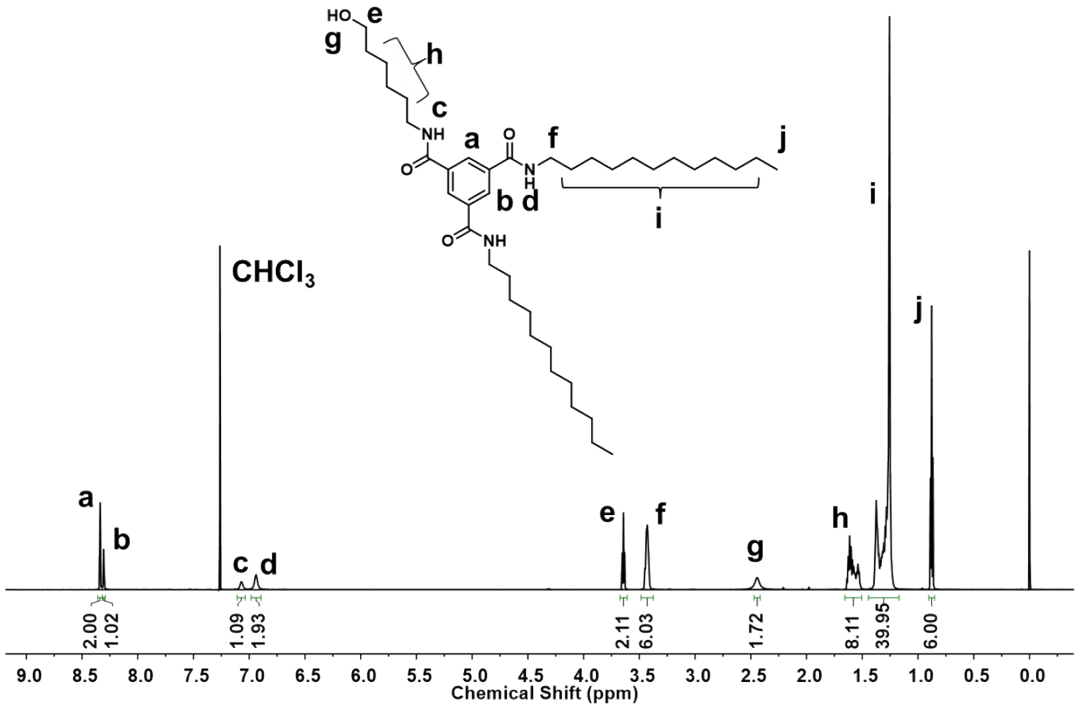

Fig. S10 ^{1}H NMR spectrum of BTA-C_6-C_{12}.

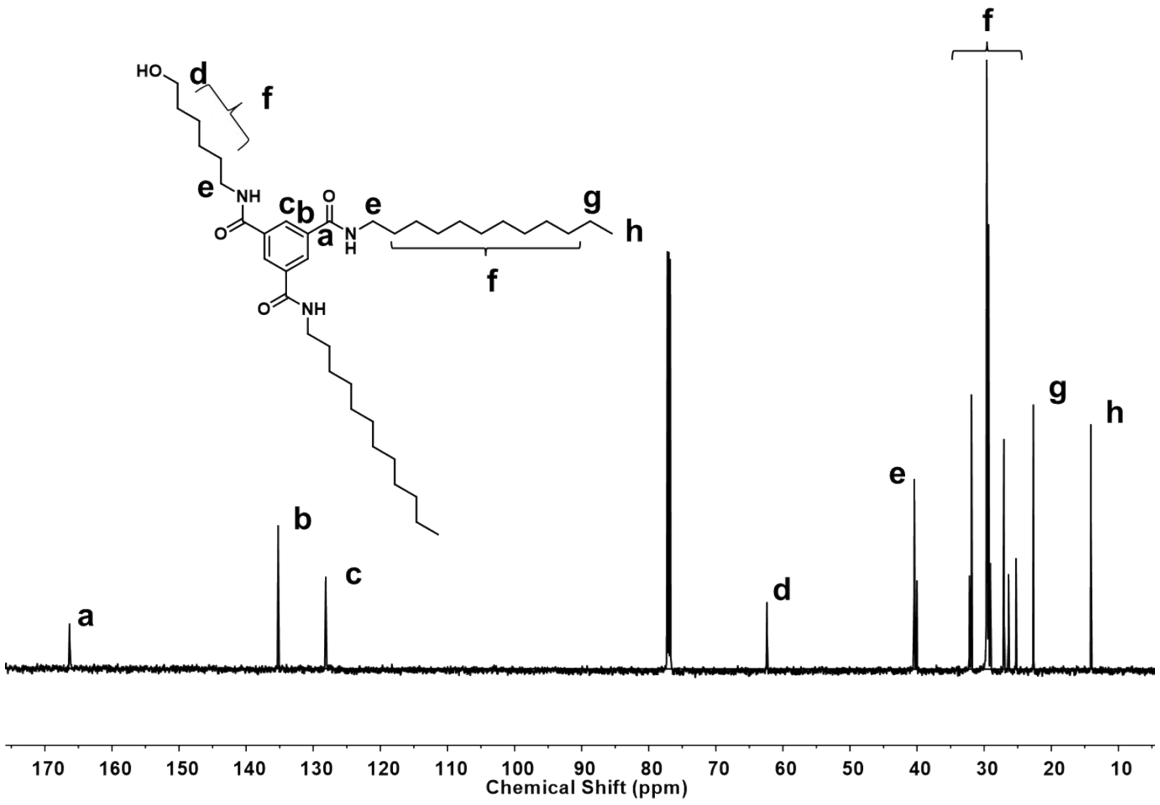

Fig. S11 ^{13}C NMR spectrum of BTA-C_6-C_{12}.

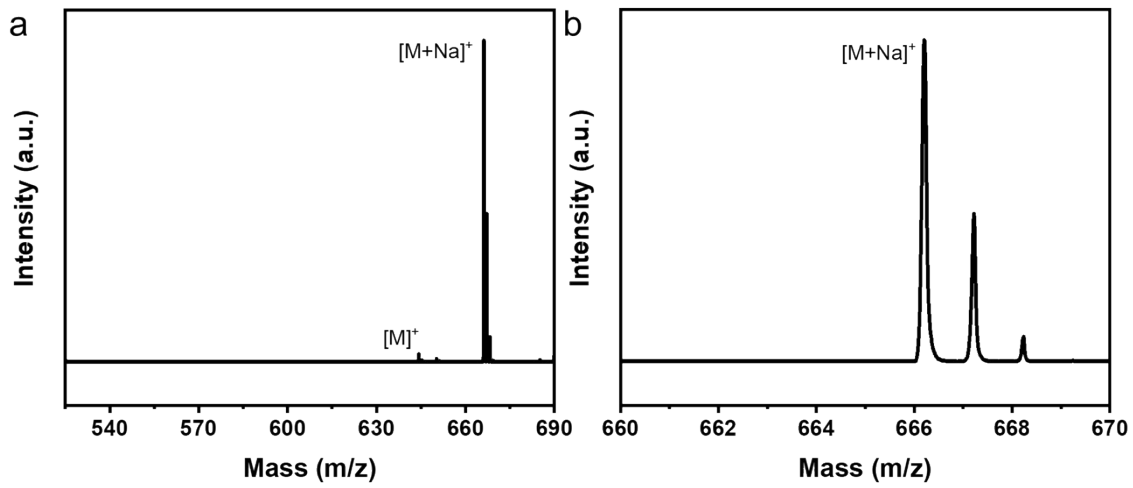

Fig. S12 MALDI-TOF mass spectra of BTA-C_6-C_{12}. (a) The overview of the spectrum and (b) the zoom-in view of the spectrum.

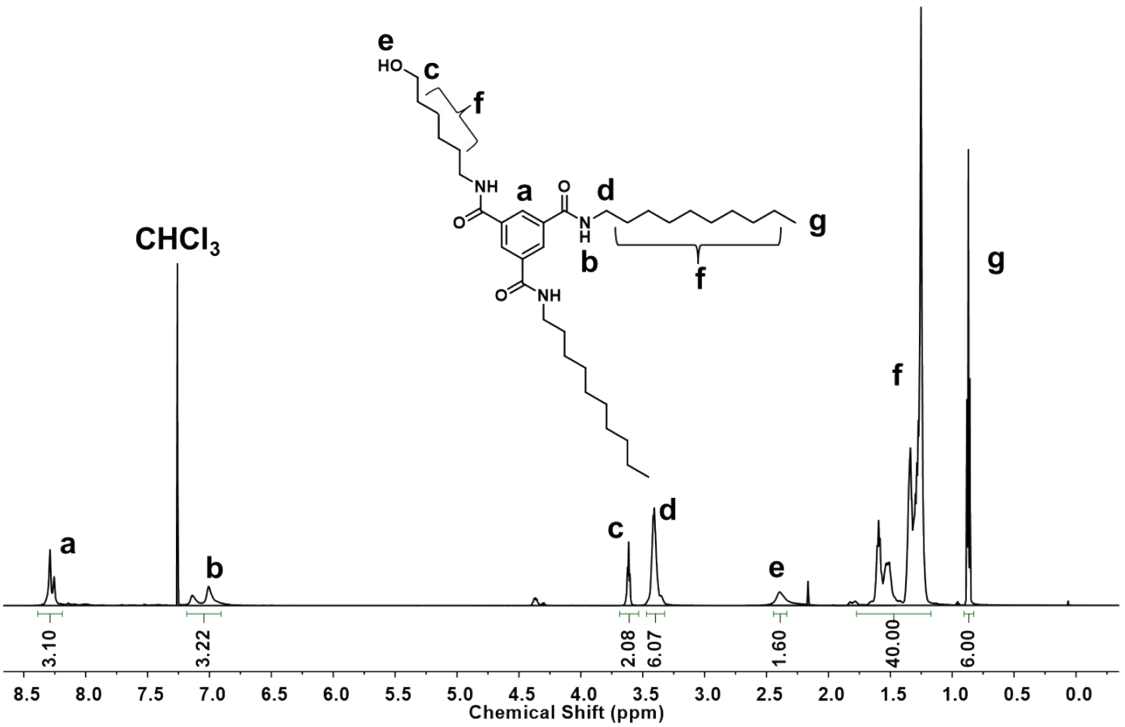

Fig. S13 ^{1}H NMR spectrum of BTA-C_6-C_{10}.

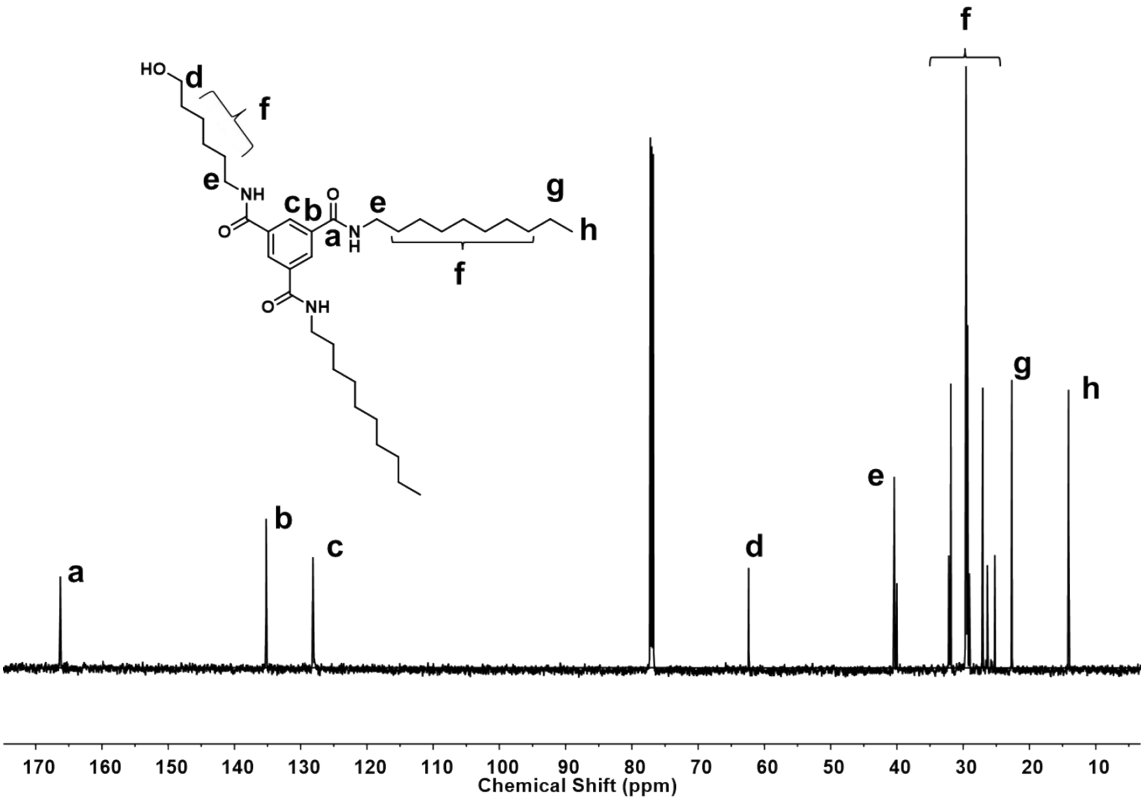

Fig. S14 ^{13}C NMR spectrum of BTA-C_6-C_{10}.

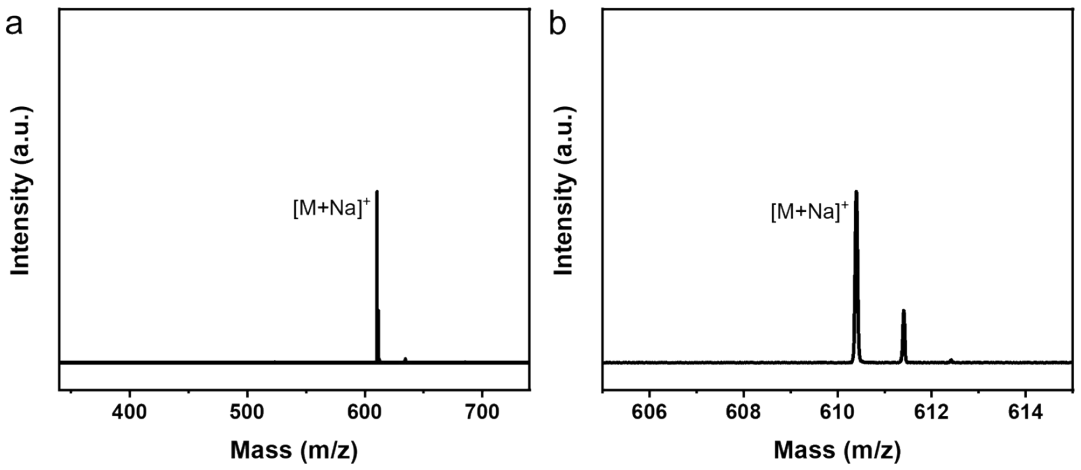

Fig. S15 MALDI-TOF mass spectra of BTA-C_6-C_{10}. a) The overview of the spectrum and b) the zoom-in view of the spectrum.

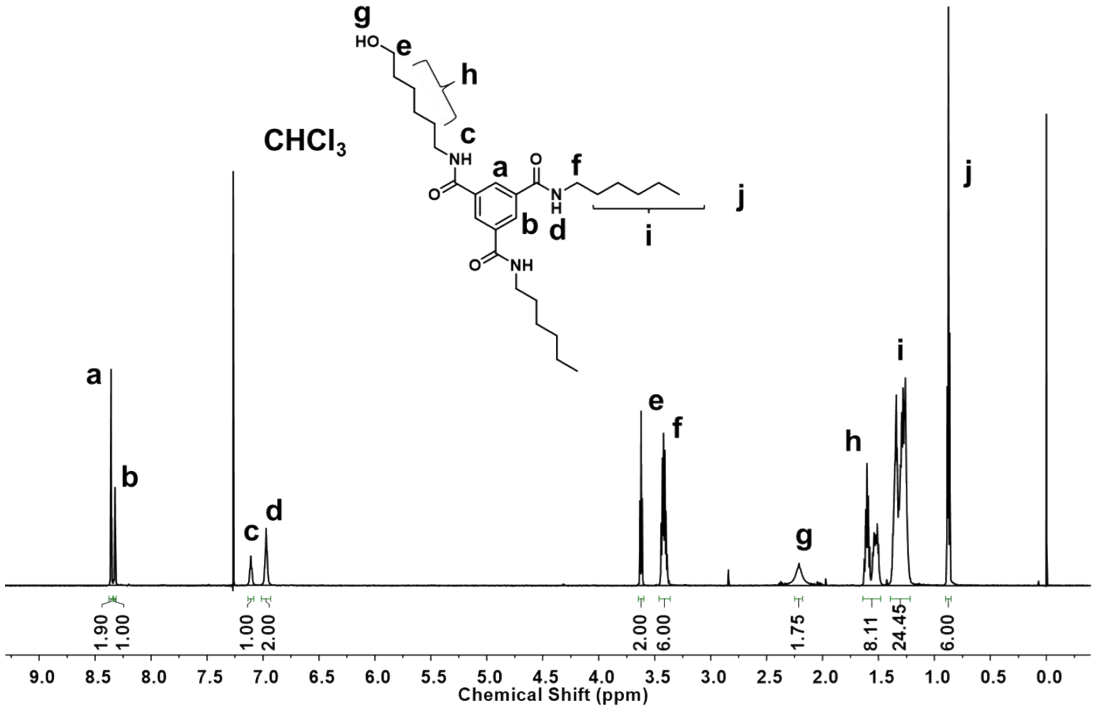

Fig. S16 ^{1}H NMR spectrum of BTA-C_6-C_8.

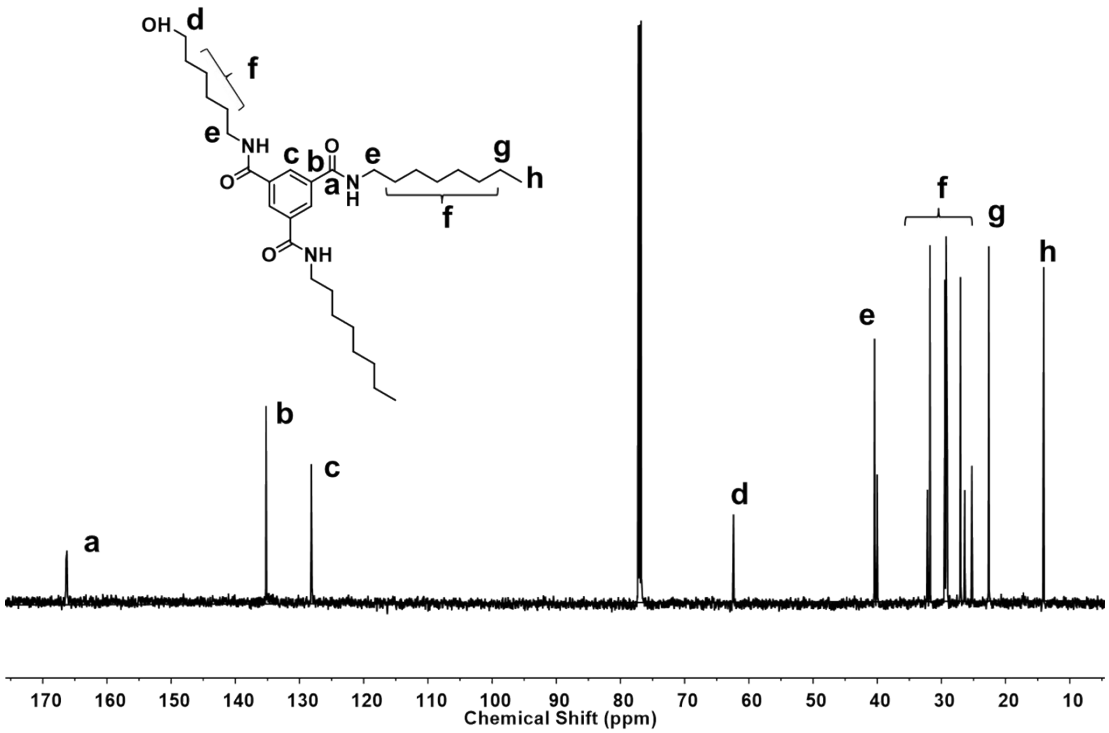

Fig. S17 ^{13}C NMR spectrum of BTA-C_6-C_8.

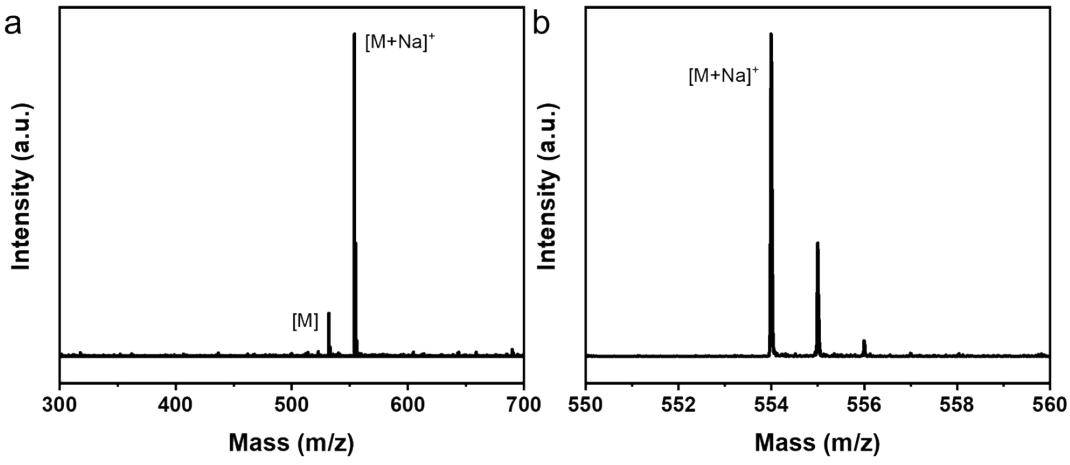

Fig. S18 MALDI-TOF mass spectra of BTA-C_6-C_8. (a) The overview of the spectrum and (b) the zoom-in view of the spectrum.

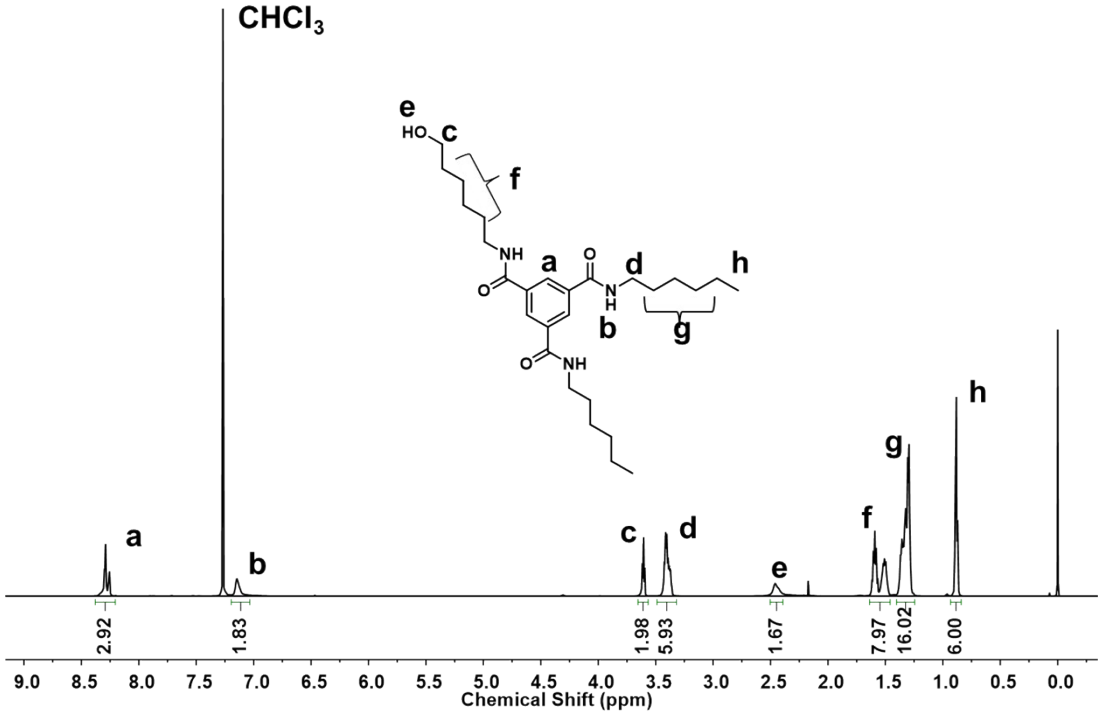

Fig. S19 ^{1}H NMR spectrum of BTA-C_6-C_6.

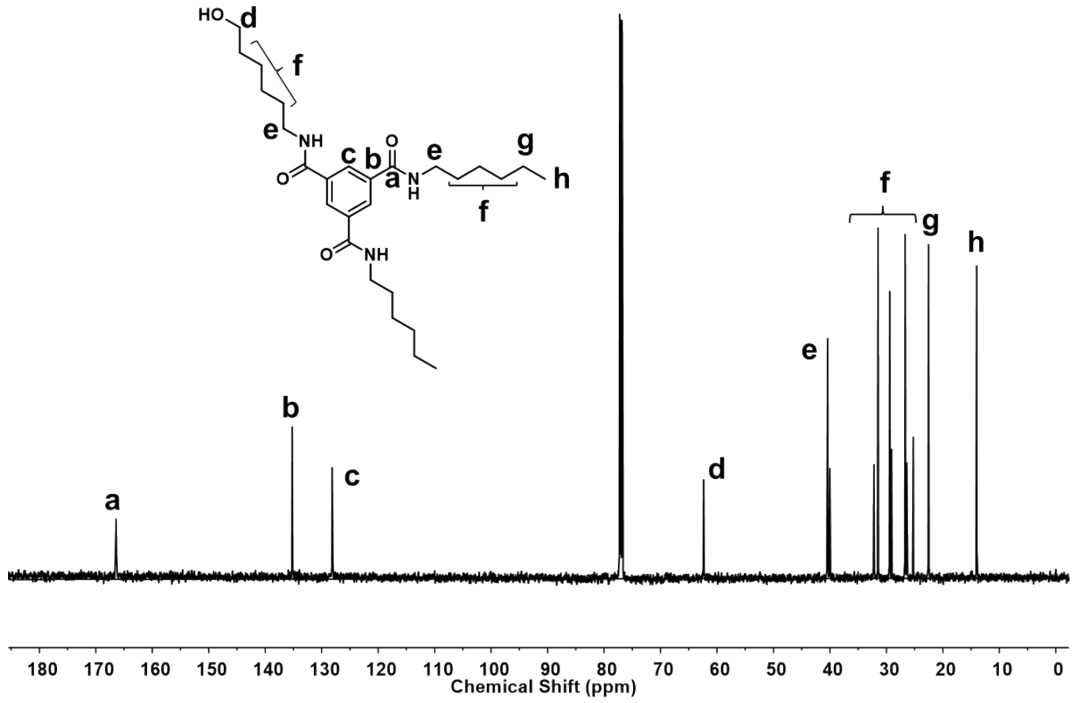

Fig. S20 ^{13}C NMR spectrum of BTA-C_6-C_6.

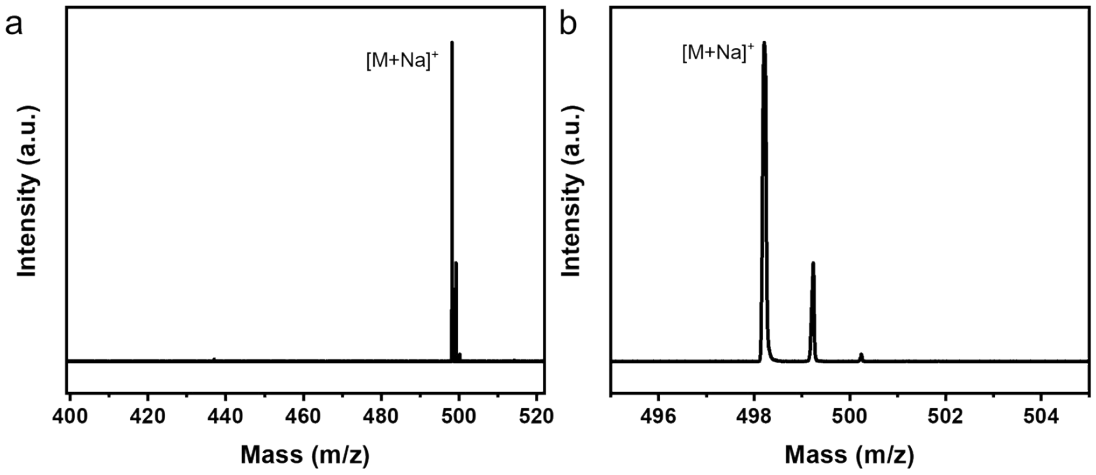

Fig. S21 MALDI-TOF mass spectra of BTA-C_6-C_6. (a) The overview of the spectrum and (b) the zoom-in view of the spectrum.

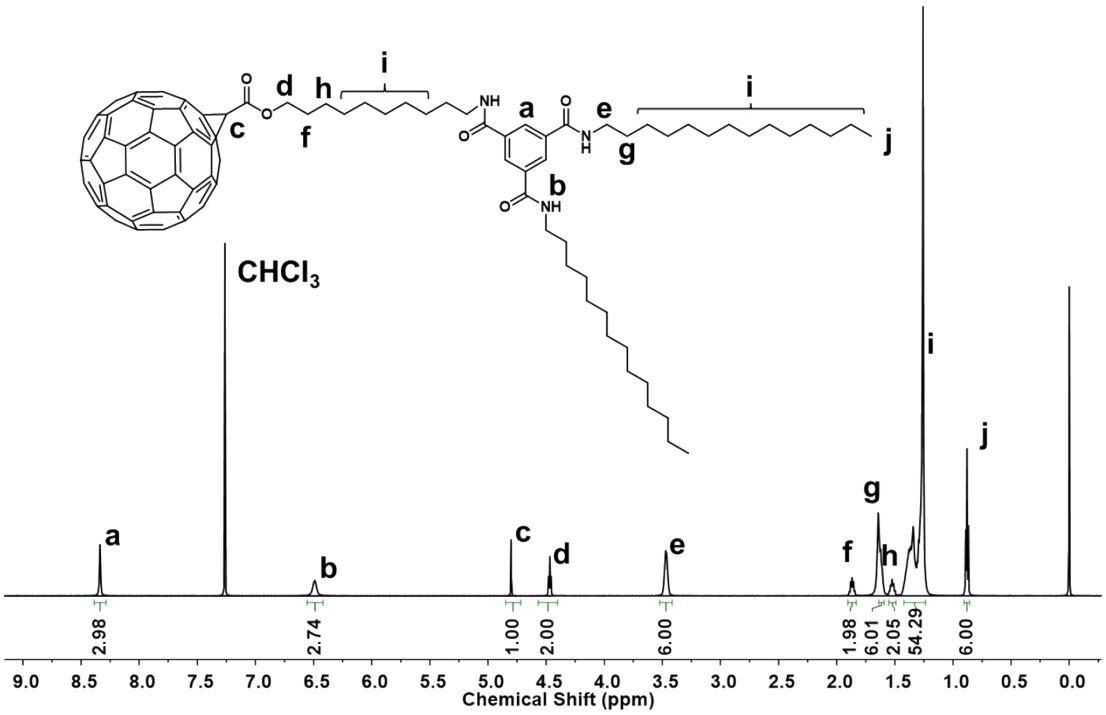

Fig. S22 ^{1}H NMR spectrum of C_{60}-C_{10}-C_{14}.

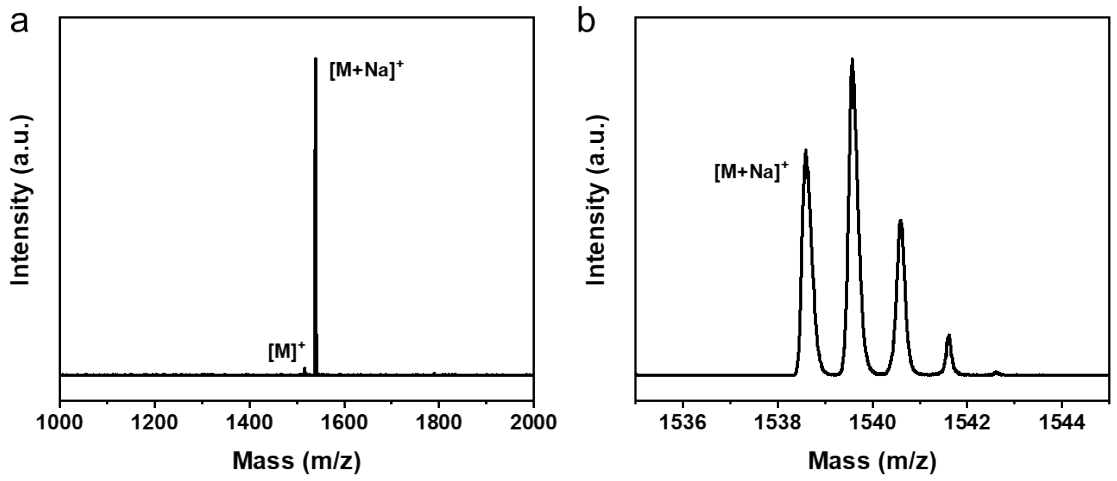

Fig. S23 MALDI-TOF mass spectra of C_{60}-C_{10}-C_{14}. (a) The overview of the spectrum and (b) the zoom-in view of the spectrum.

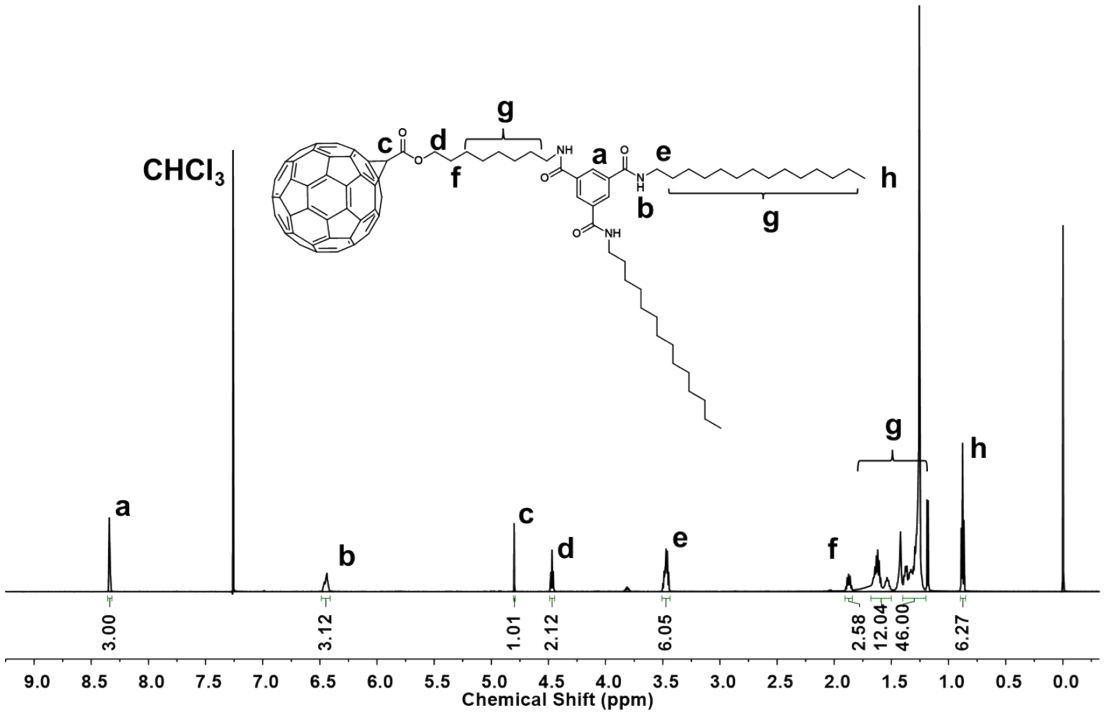

Fig. S24 ^{1}H NMR spectrum of C_{60}-C_8-C_{14}.

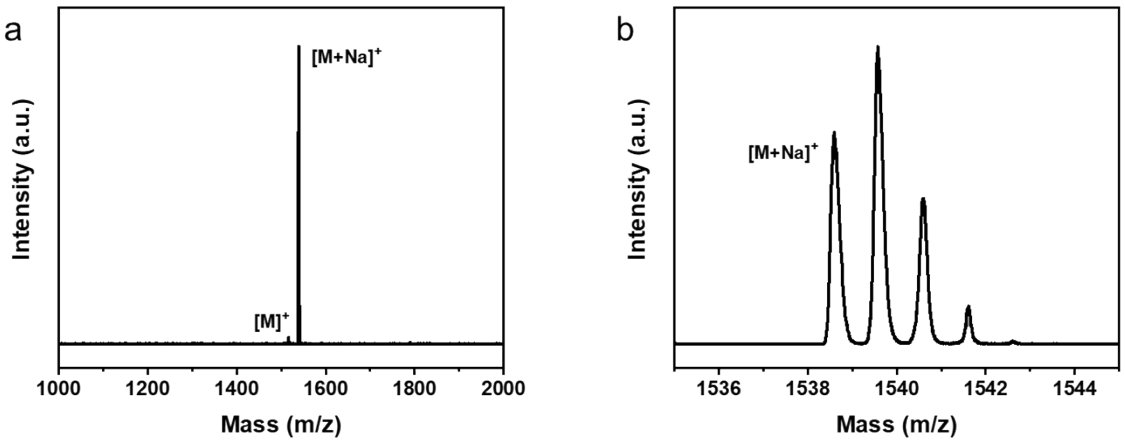

Fig. S25 MALDI-TOF mass spectra of C_{60}-C_8-C_{14}. (a) The overview of the spectrum and (b) the zoom-in view of the spectrum.

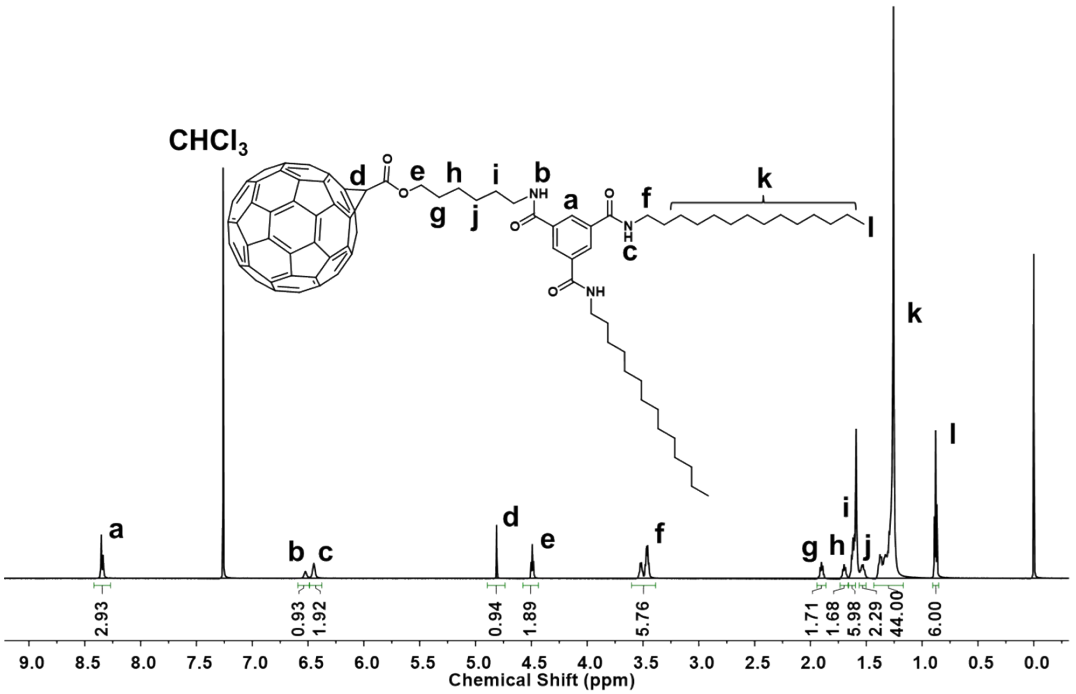

Fig. S26 ^{1}H NMR spectrum of C_{60}-C_6-C_{14}.

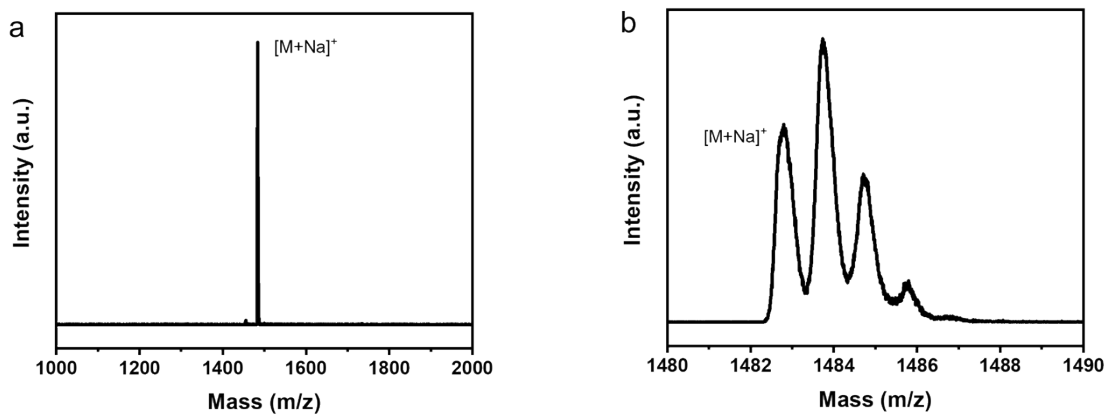

Fig. S27 MALDI-TOF mass spectra of C_{60}-C_6-C_{14}. (a) The overview of the spectrum and (b) the zoom-in view of the spectrum.

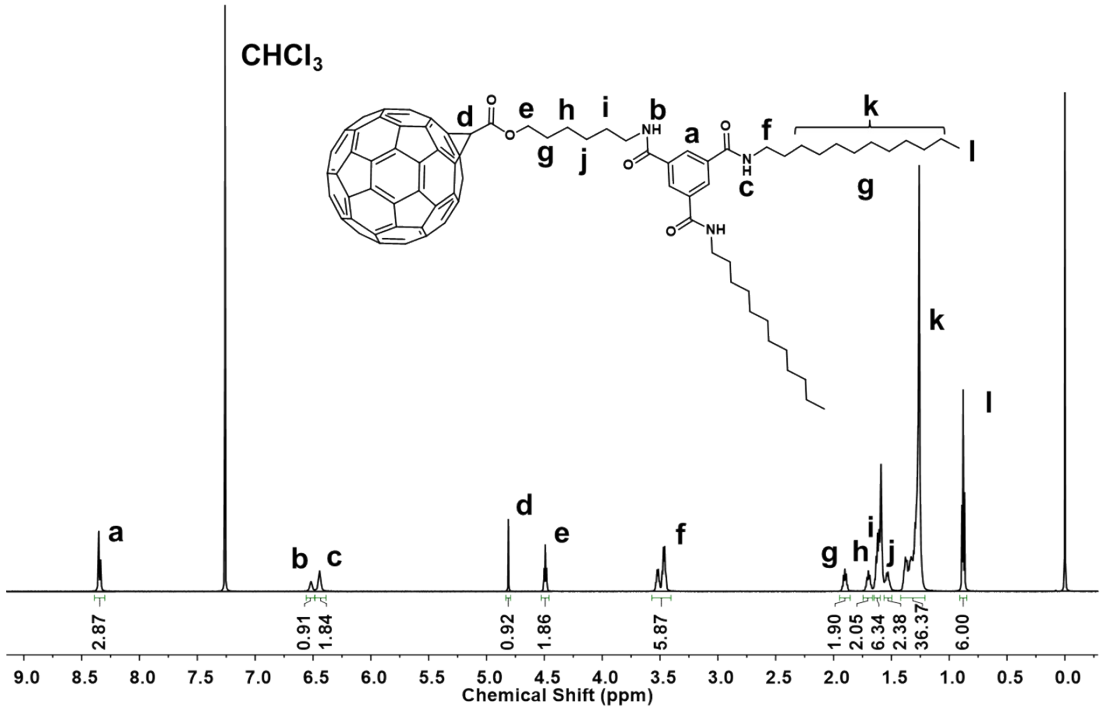

Fig. S28 ^{1}H NMR spectrum of C_{60}-C_6-C_{12}.

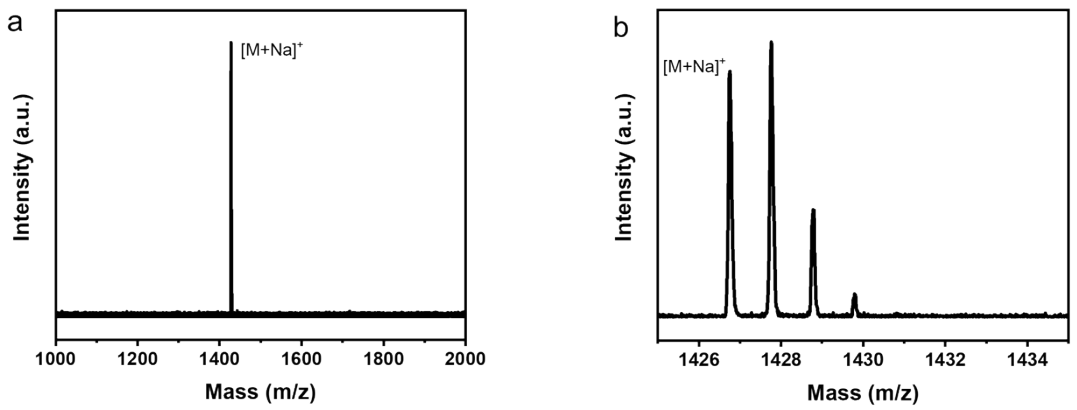

Fig. S29 MALDI-TOF mass spectra of C_{60}-C_6-C_{12}. (a) The overview of the spectrum and (b) the zoom-in view of the spectrum.

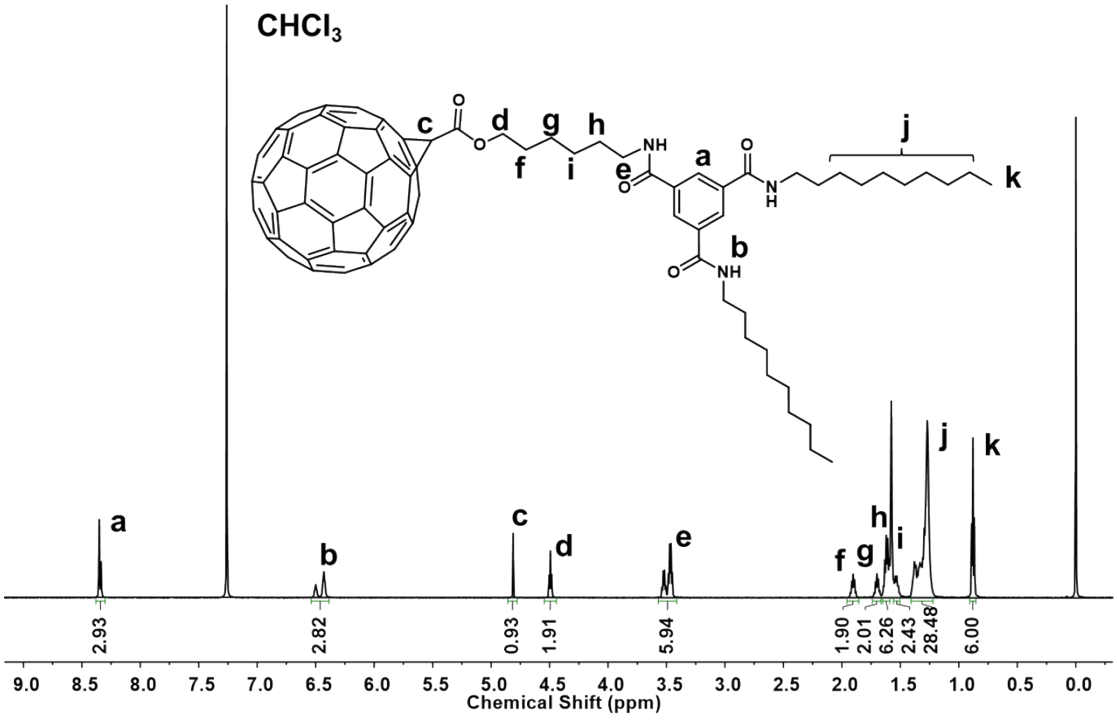

Fig. S30 ^{1}H NMR spectrum of C_{60}-C_6-C_{10}.

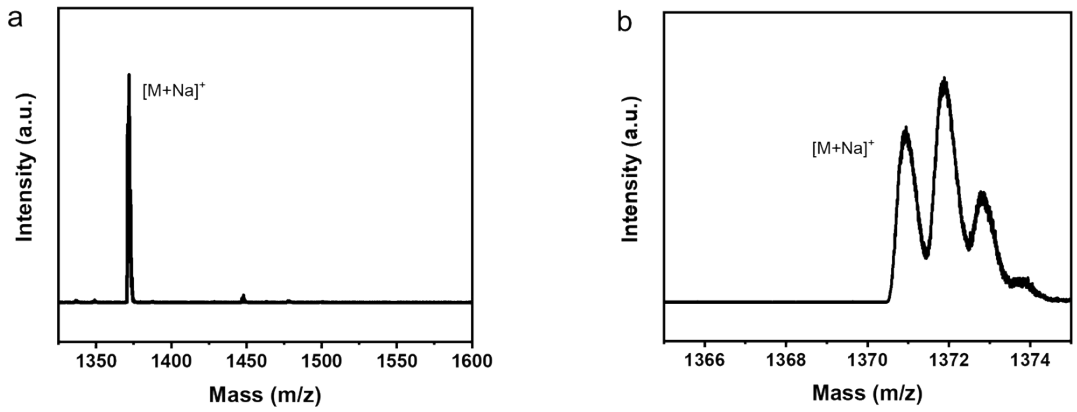

Fig. S31 MALDI-TOF mass spectra of C_{60}-C_6-C_{10}. (a) The overview of the spectrum and (b) the zoom-in view of the spectrum.

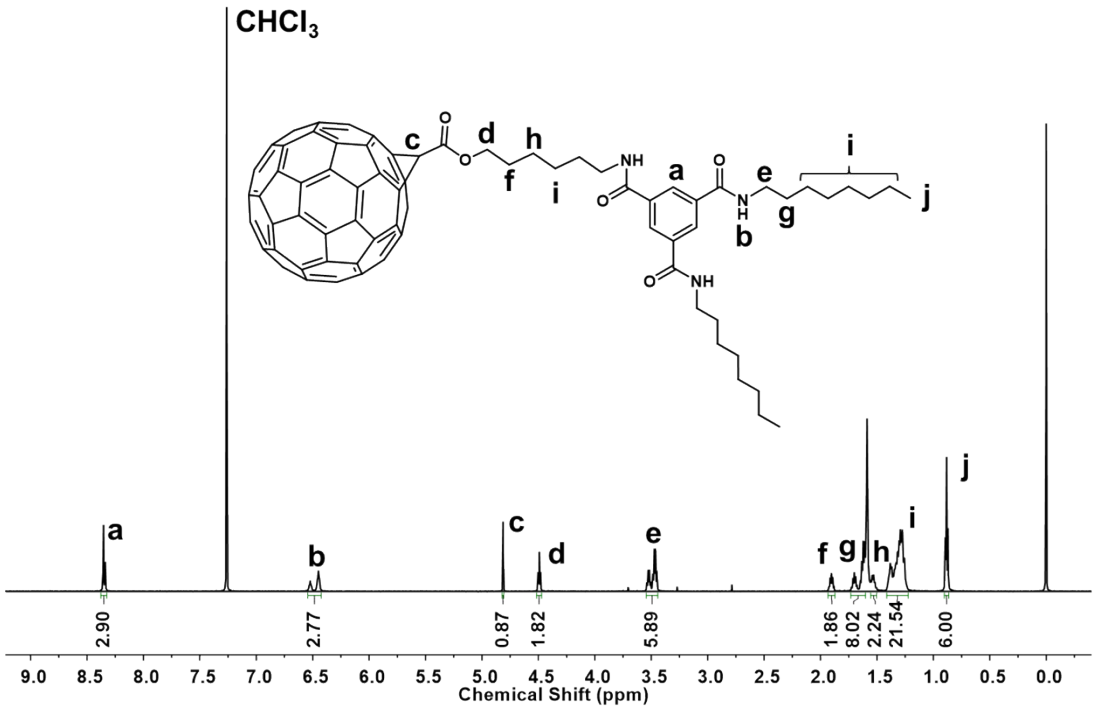

Fig. S32 ^{1}H NMR spectrum of C_{60}-C_6-C_8.

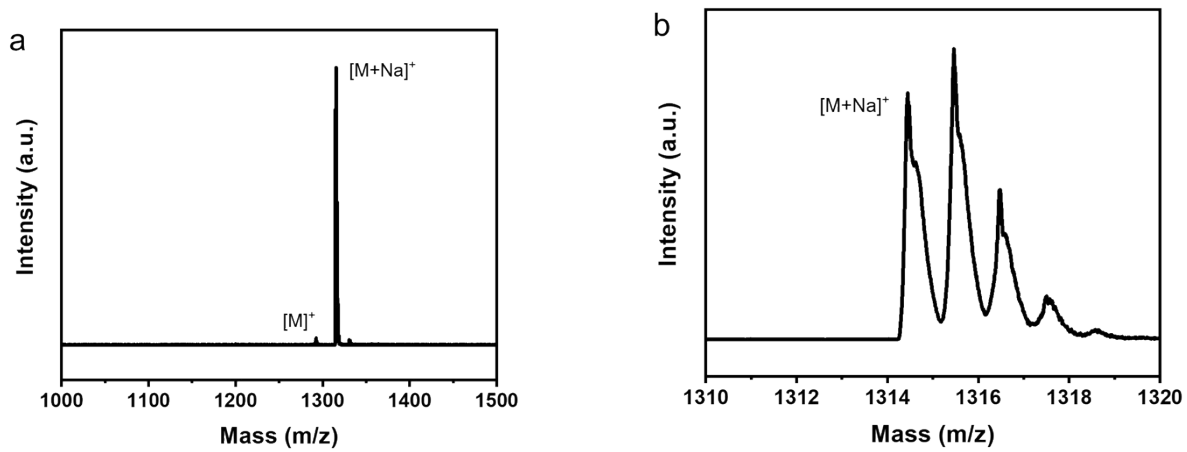

Fig. S33 MALDI-TOF mass spectra of C_{60}-C_6-C_8. (a) The overview of the spectrum and (b) the zoom-in view of the spectrum.

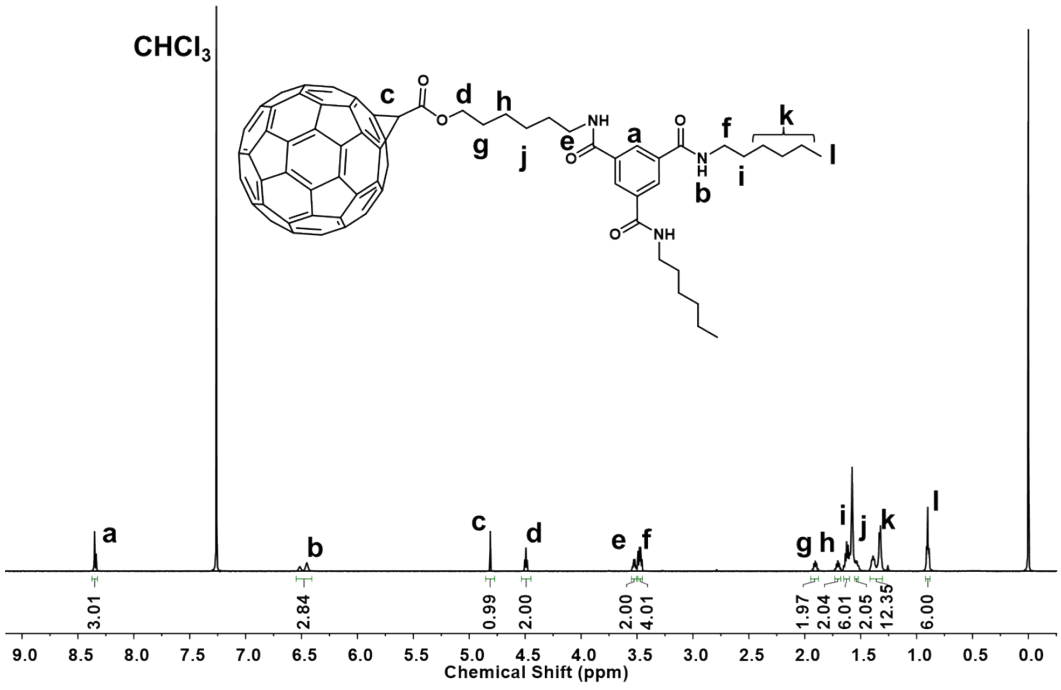

Fig. S34 ^{1}H NMR spectrum of C_{60}-C_6-C_6.

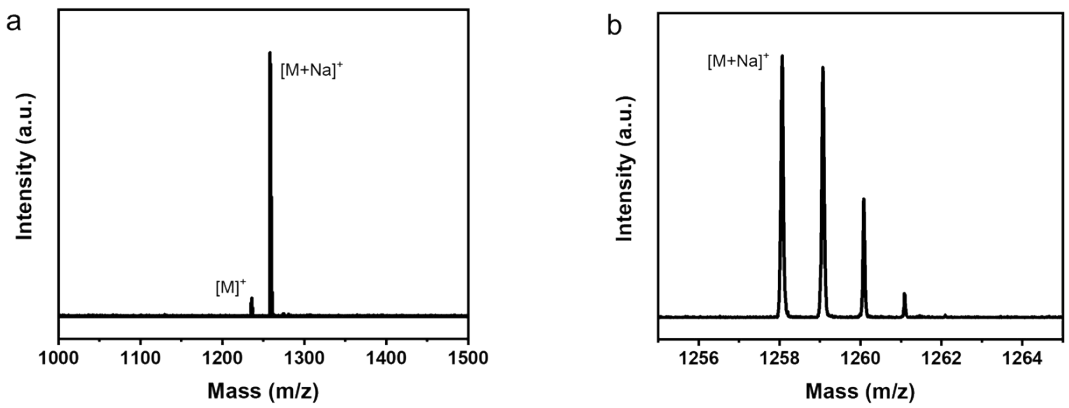

Fig. S35 MALDI-TOF mass spectra of C_{60}-C_6-C_6. (a) The overview of the spectrum and (b) the zoom-in view of the spectrum.

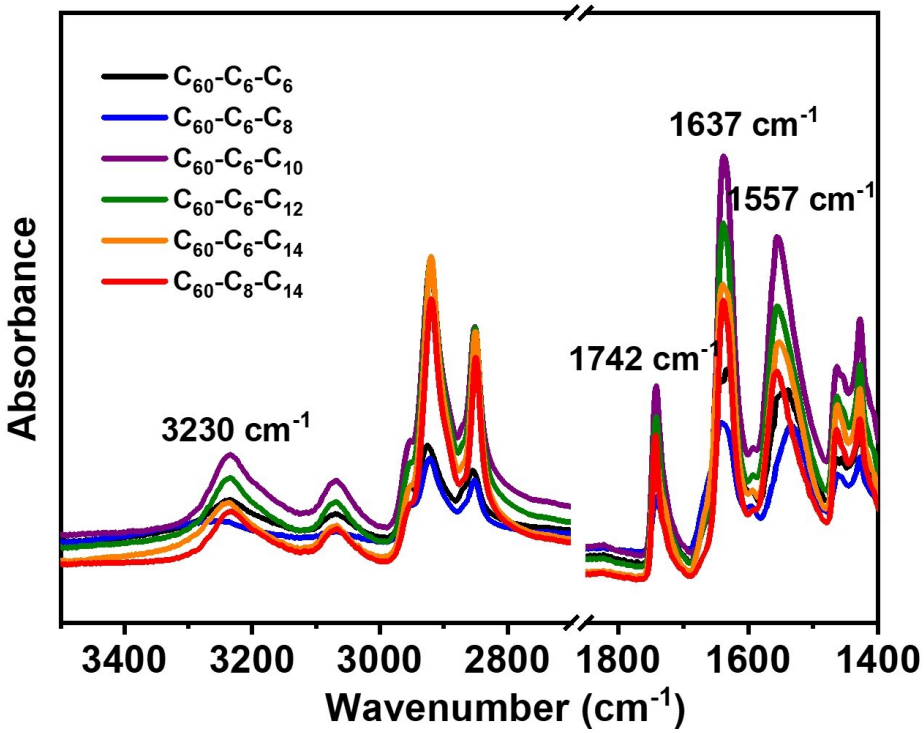

Fig. S36 FTIR spectra of C_{60}-C_m-C_n.

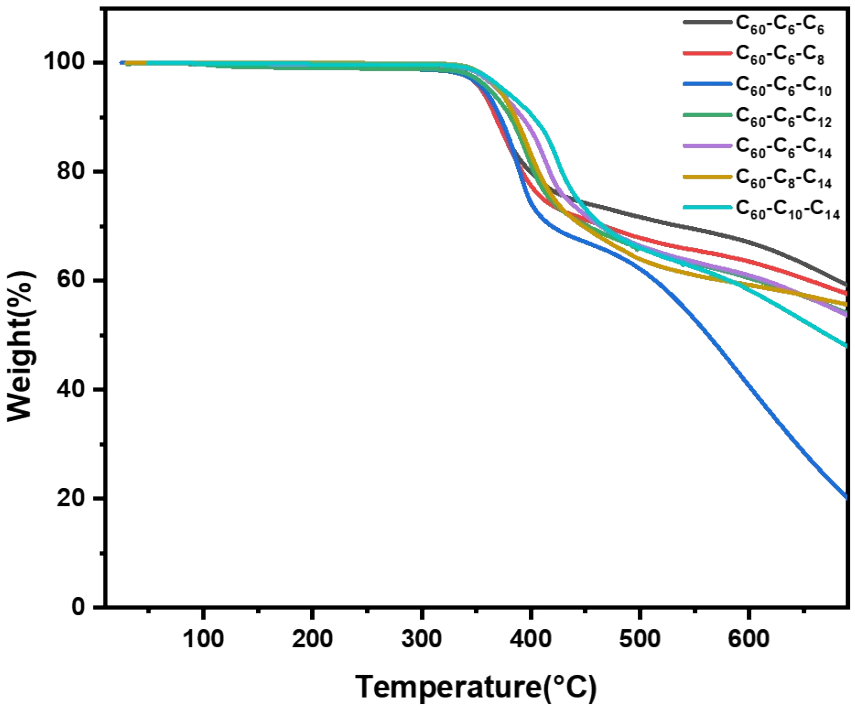

Fig. S37 TGA curves of C_{60}-C_m-C_n.

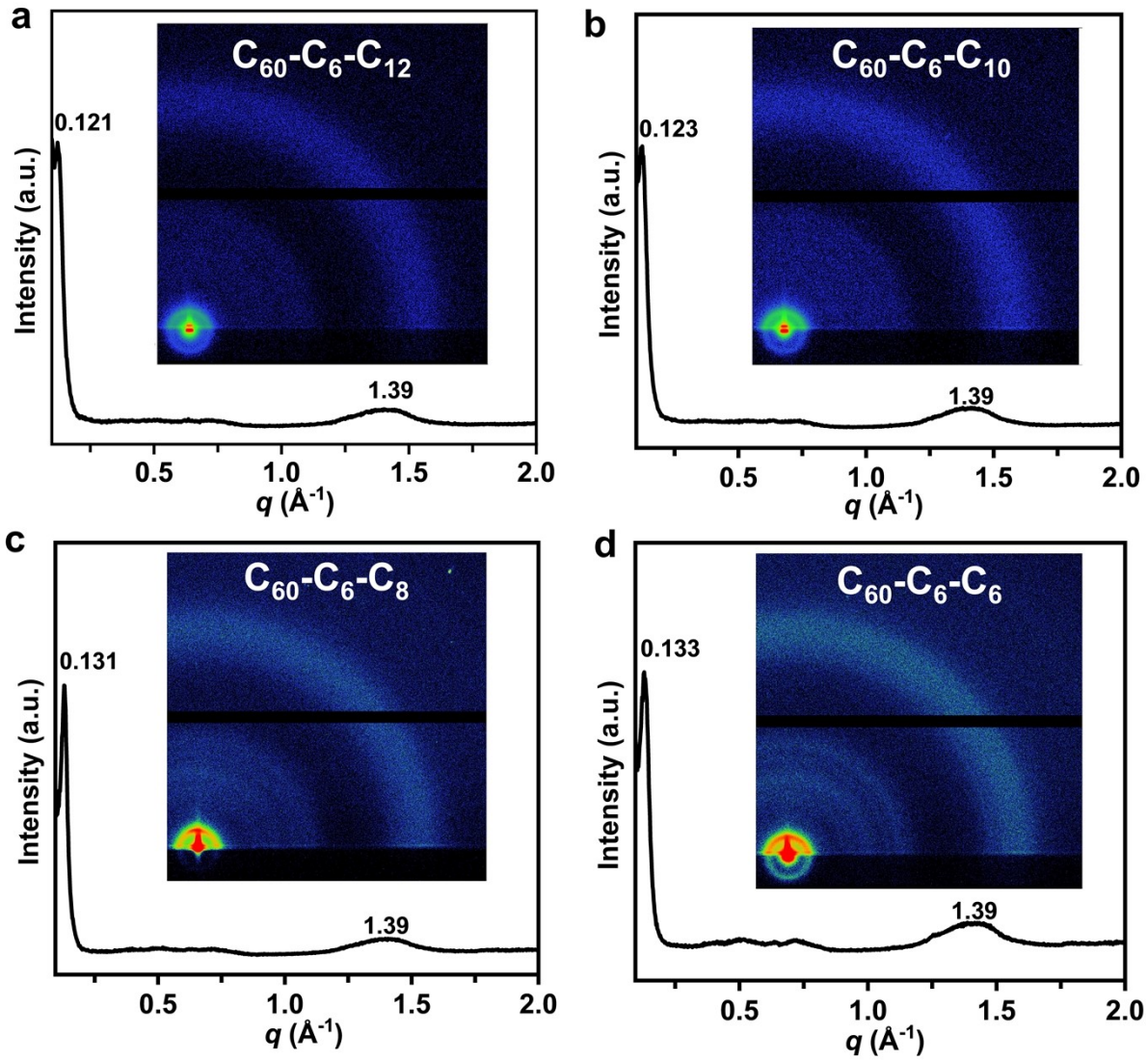

Fig. S38 1D SAXS curves and corresponding 2D GI-SAXS images of superstructures formed by C_{60}-C_6-C_{12} (a), C_{60}-C_6-C_{10} (b), C_{60}-C_6-C_8 (c) and C_{60}-C_6-C_6 (d) in toluene/isopropanol (1/1, v/v) at 25 °C.

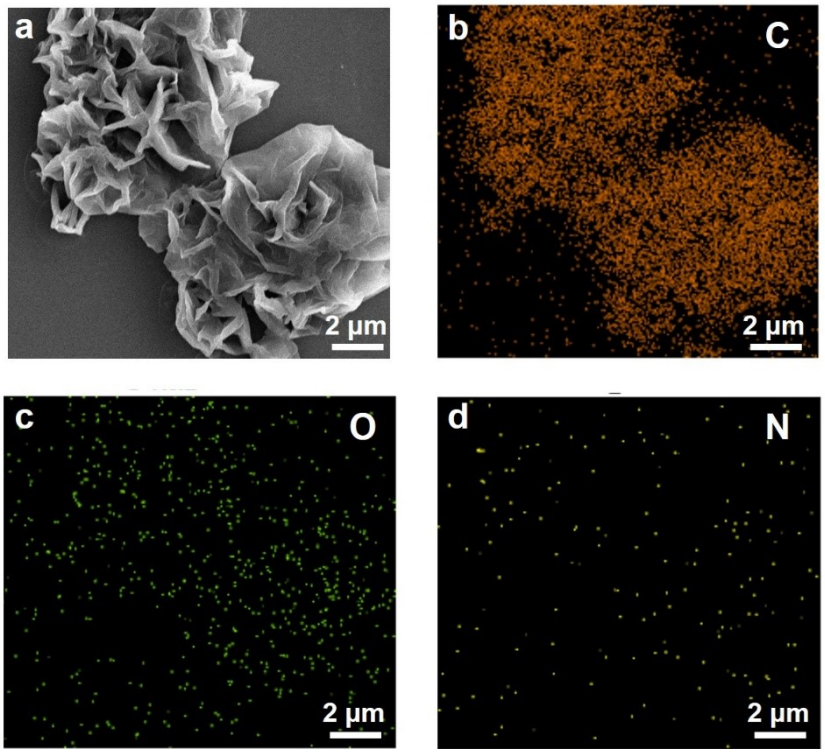

Fig. S39 SEM image (a) of the flower-like assemblies of C_{60}-C_{10}-C_{14} in toluene/isopropanol (1/1, v/v) and corresponding EDS mapping of element C (b), O (c) and N (d).

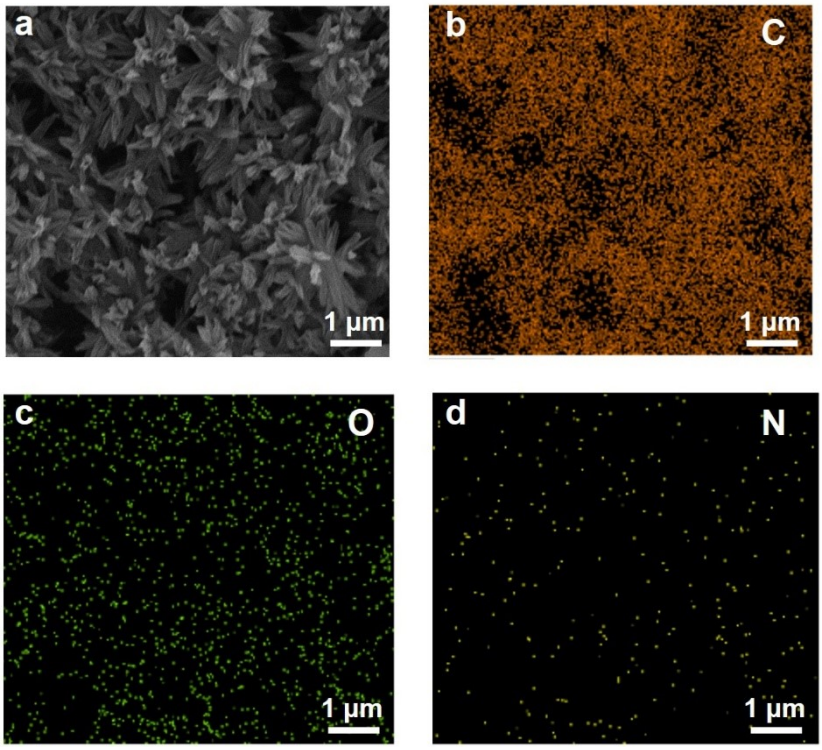

Fig. S40 SEM image (a) of the rod-like assemblies of C_{60}-C_6-C_6 in toluene/isopropanol (1/1, v/v) and corresponding EDS mapping of element C (b), O (c) and N (d).

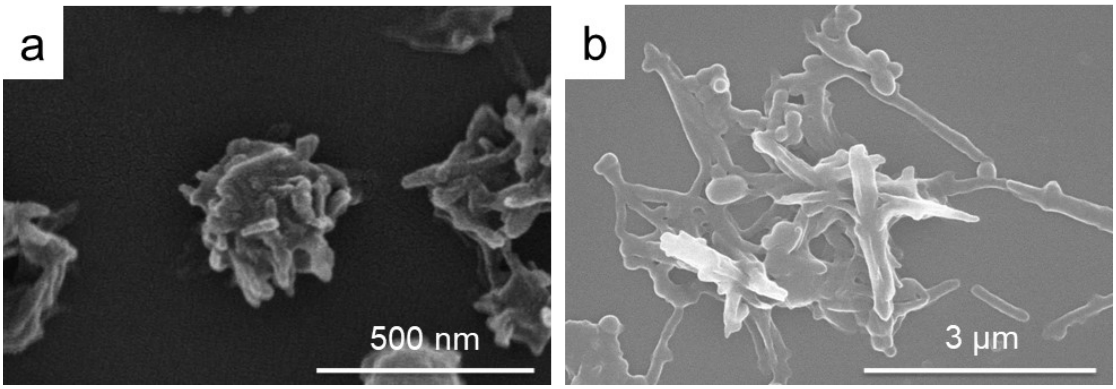

Fig. S41 SEM images of the self-assembled superstructures of C_{60}-C_6-C_{12} in toluene/isopropanol (1:2) (a) and (1:5) (b).

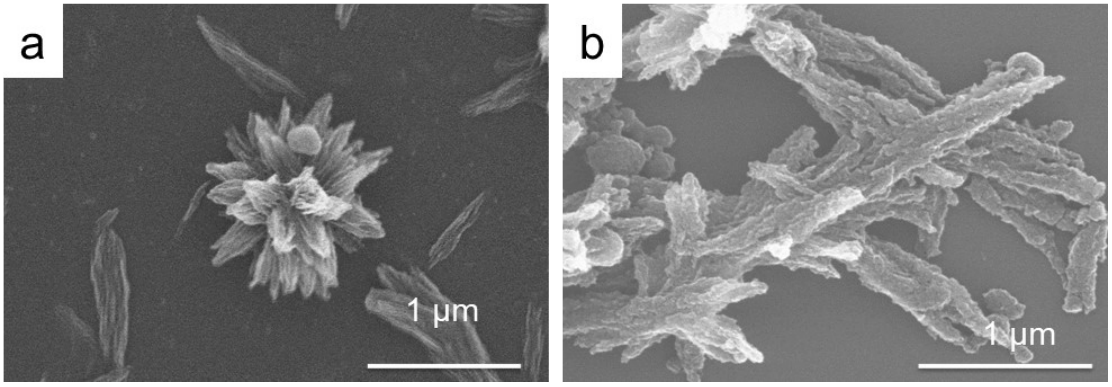

Fig. S42 SEM images of the self-assembled superstructures of C_{60}-C_6-C_{10} in toluene/isopropanol (1:2) (a) and (1:5) (b).

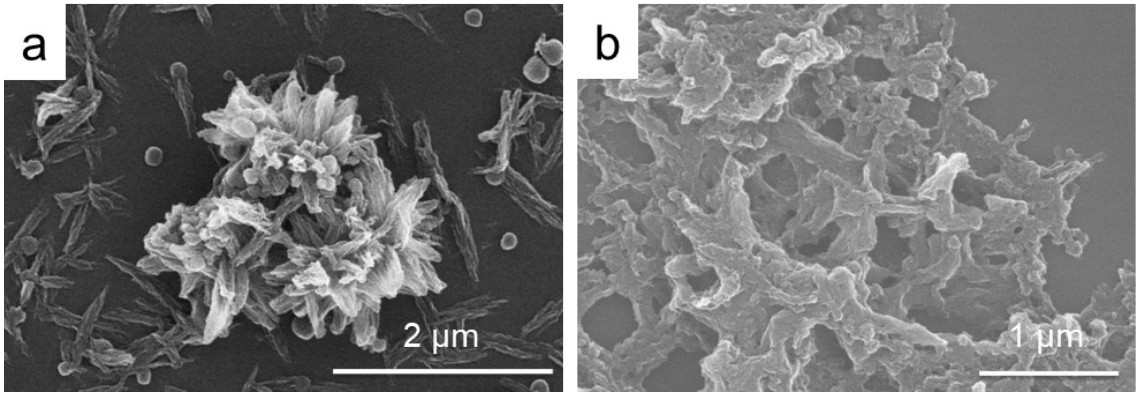

Fig. S43 SEM images of the self-assembled superstructures of C_{60}-C_6-C_8 in toluene/isopropanol (1:2) (a) and (1:5) (b).

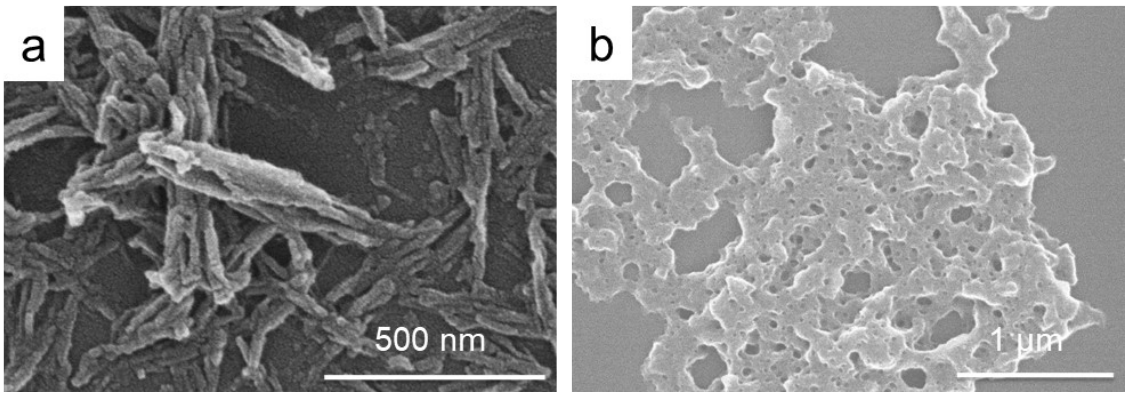

Fig. S44 SEM images of the self-assembled superstructures of C_{60}-C_6-C_6 in toluene/isopropanol (1:2) (a) and (1:5) (b).

3. References

[1] T. Tada, Y. Ishida, K. Saigo, *J. Org. Chem.* **2006**, *71* (*4*), 1633-1639.

[2] B. Ma, C. E. Bunker, R. Guduru, X.-F. Zhang, Y.-P. Sun, *J. Phys. Chem. A* **1997**, *101* (*31*), 5626-5632.